Forest-atmosphere exchange of reactive nitrogen in a remote region – Part II: Modeling annual budgets

Pascal Wintjen[1], Frederik Schrader[1], Martijn Schaap[2,3], Burkhard Beudert[4], Richard Kranenburg[2], and Christian Brümmer[1]

[1]Thünen Institute of Climate-Smart Agriculture, Bundesallee 68, 38116 Braunschweig, Germany
[2]TNO, Climate Air and Sustainability, Utrecht, 3584 CB, The Netherlands
[3]Institute of Meteorology, Freie Universität Berlin, 12165 Berlin, Germany
[4]Bavarian Forest National Park, 94481, Grafenau, Germany

Correspondence to: Pascal Wintjen (pascal.wintjen@thuenen.de)

Abstract. To monitor the effect of current nitrogen emissions and mitigation strategies, total atmospheric nitrogen deposition to forests is commonly estimated using chemical transport models or canopy budget models in combination with throughfall measurements. Since flux measurements of reactive nitrogen (N_r) compounds are scarce, dry deposition process descriptions as well as the calculated flux estimates and annual budgets are subject to considerable uncertainties. In this study, we compared four different approaches to quantify annual dry deposition budgets of total reactive nitrogen (ΣN_r) at a mixed forest site situated in the Bavarian Forest National Park, Germany. Dry deposition budgets were quantified based on (I) 2.5 years of eddy-covariance flux measurements with the Total Reactive Atmospheric Nitrogen Converter (TRANC), (II) an in-situ application of the bidirectional inferential resistance scheme DEPAC (Deposition of Acidifying Compounds), here called DEPAC-1D, (III) a simulation with the chemical transport model LOTOS-EUROS (LOng Term Ozone Simulation – EURopean Operational Smog) v2.0 using DEPAC as dry deposition module, and (IV) a canopy budget technique (CBT).

Averaged annual ΣN_r dry deposition estimates determined from TRANC measurements were 4.7±0.2 and 4.3±0.4 kg N ha^{-1} a^{-1} using DEPAC-1D only, and the Mean-Diurnal-Variation method in combination with DEPAC-1D as gap-filling approaches, respectively. DEPAC-1D modeled dry deposition, using concentrations and meteorological drivers measured at the site, was 5.8±<0.1 kg N ha^{-1} a^{-1}. In comparison to TRANC fluxes, DEPAC-1D estimates were systematically larger during summer, and in close agreement in winter. Modeled ΣN_r deposition velocities (v_d) of DEPAC-1D were found to increase with lower temperatures, higher relative humidity, and in the presence of wet leaf surfaces, in particular from May to September. This observation was in contradiction to TRANC-observed fluxes, leading to the conclusion that the parametrizations may need revision. LOTOS-EUROS modeled annual dry deposition was 6.5±0.3 kg N ha^{-1} a^{-1} for the site-specific weighting of land-use classes within the site's grid cell. LOTOS-EUROS showed substantial discrepancies to measured ΣN_r deposition during spring and winter, which was related to an overestimation of ammonia concentrations within the grid cell. LOTOS-EUROS predicted an averaged ΣN_r concentration of 5.0±3.3 µg N m^{-3}. Ammonia (NH_3) contributed most to modeled ΣN_r concentrations but the modeled NH_3 concentrations were overestimated by a factor two to three compared to measured values. Annual deposition estimates were in the range of minimum and maximum estimates determined from CBT being at 3.8±0.5 and 6.7±0.3 kg N ha^{-1} a^{-1}, respectively. By adding locally measured wet-only deposition, we estimated an annual total nitrogen deposition input between 11.5 and 14.8 kg N ha^{-1} a^{-1}, which is at the upper end of the critical load ranges proposed for deciduous and coniferous forests.

In this work, we conducted one of the first comparisons of micrometeorological and ecological methods for estimating annual nitrogen dry deposition to a remote mixed forest.

1 Introduction

40 In the last century, global nitrogen emissions have increased significantly due to anthropogenic activities (Fowler et al., 2013). Reactive nitrogen compounds, such as ammonia (NH_3) and nitrogen oxides (NO_x), contribute most to the emissions. Ammonia emissions originate mostly from animal husbandry and fertilizer application (Sutton et al., 2011, 2013), whereas NO_x emissions are mainly related to combustion processes in, e.g., transport and industry (Erisman et al., 2011, 2013). Although fertilizer use and the internal combustion engine are vital for world's food security and the economy, the release of these compounds into

45 the atmosphere has a wide range of negative effects (Krupa, 2003; Galloway et al., 2003; Erisman et al., 2013). Deposition of reactive nitrogen into ecosystems has been identified as a reduction factor for biodiversity (Bobbink et al., 1998; Krupa, 2003; Galloway et al., 2003; Sutton et al., 2011). Especially ecosystems at nutrient poor soils are highly sensitive to additional nitrogen inputs resulting in a change in plant species (Damgaard et al., 2011; Paulissen et al., 2016) and species composition in forests (Dirnböck et al., 2014, 2018; Roth et al., 2022). Critical loads are used to show at which level long term nitrogen

50 deposition may lead to adverse impacts (Hettelingh et al., 1995). Investigations by Hettelingh et al. (2013) have shown that half of the European ecosystems receive nitrogen above the critical load level. In Germany, the fraction of ecosystems with a critical load exceedance is estimated to be about 70 % (Schaap et al., 2018).

Quantitative estimation of the total nitrogen deposition is needed to assess exceedances of critical loads and to develop

55 successful mitigation strategies. Although wet deposition is relatively straightforward to measure, the accurate quantification of dry N deposition remains a challenge. Recent progress in fast and robust measurement techniques allowed to investigate the temporal dynamics in concentrations and dry deposition fluxes (using the eddy-covariance (EC) approach) for total reactive nitrogen (ΣN_r) (Marx et al., 2012; Ammann et al., 2012; Brümmer et al., 2013, 2022; Zöll et al., 2019; Ammann et al., 2019; Wintjen et al., 2020, 2022) and its individual compounds, e.g. for NH_3 (Ferrara et al., 2012, 2021; Zöll et al., 2016; Moravek

60 et al., 2020). For ΣN_r, the total reactive atmospheric nitrogen converter (TRANC) (Marx et al., 2012) coupled to a chemiluminescence detector (CLD) has shown its suitability for flux measurements in various field applications (see references for ΣN_r above). Despite the recent progress, the number and temporal coverage of available datasets remains small. As these in-situ measurements are only valid for the ecosystem where the specific observations took place, a large-scale assessment based on observations alone is not possible.

65

Chemical transport models (CTMs) are used to assess nitrogen deposition over large regions. For Germany, the CTM LOTOS-EUROS (Wichink Kruit et al., 2012; Manders et al., 2017; van der Graaf et al., 2020) is applied for the mapping of nitrogen deposition fluxes across the country. LOTOS-EUROS predicts the dry deposition of various N_r compounds, namely nitrogen dioxide (NO_2), nitric oxide (NO), nitric acid (HNO_3), ammonia (NH_3), and particulate ammonium (NH_4^+) and nitrate (NO_3^-),

70 in each grid cell by utilizing meteorological data from the European Centre for Medium Range Weather Forecasts (ECMWF), modeled concentrations of the mentioned compounds based on their emission sources and chemical processing, as well as information about the land-use distribution within each grid cell. The deposition module DEPAC (Deposition of Acidifying Compounds) is applied for calculating dry deposition velocities of those compounds (Erisman et al., 1994). DEPAC is a dry deposition inferential scheme featuring bidirectional NH_3 exchange (van Zanten et al., 2010; Wichink Kruit et al., 2012), which

75 is also implemented in the Operational Priority Substance (OPS) model (van Jaarsveld, 2004; Sauter et al., 2020). DEPAC can be used as stand-alone model for estimating dry deposition of N_r compounds. For site-based modeling with DEPAC, decoupled from a CTM and henceforth called DEPAC-1D, only measurements of common micrometeorological variables and concentrations of the individual N_r compounds are needed. In the past, deposition estimates have often been obtained through such an inferential modeling approach (Flechard et al., 2011, 2020; Li et al., 2016; Schwede et al., 2011).

80

To evaluate modeled annual total dry deposition and seasonal patterns in modeled fluxes and deposition velocities, a careful comparative analysis to flux measurements may provide feedback on the representativeness of the input data and the bidirectional parametrizations (Wichink Kruit et al., 2010; Wichink Kruit et al., 2017). Wintjen et al. (2022) presented and analyzed novel flux measurements of ΣN_r and several subcomponents focussing on temporal dynamics above a remote, mixed forest site spanning a 2.5 year period. This dataset provides a unique opportunity for the evaluation of different approaches to quantify dry deposition fluxes. Such comparisons with novel measurement techniques are sparse and only available from few field campaigns (Ammann et al., 2012; Brümmer et al., 2013, 2022; Zöll et al., 2019). Since the adoption of the Geneva Convention on Long-Range Transboundary Air Pollution (CLRTAP) in 1979, throughfall measurements has been carried out at many sites of the International Cooperative Programmes of air pollution effects on Forests (ICP Forests, www.icp-forests.net, last access: 14 March 2022) and forested catchments (ICP Integrated Monitoring, http://www.syke.fi/nature/icpim, last access: 14 March 2022) according to standardized protocols. Using the so-called canopy budget technique (CBT) throughfall measurements also allow to give an estimate of the annual nitrogen dry deposition (Draaijers and Erisman, 1995; de Vries et al., 2003).

In this study, we provide a comparison of four independent methods for estimating nitrogen dry deposition for a remote mixed forest site in the Bavarian Forest National Park. The comparison is made for a 2.5 year period for which novel flux measurements were available (see companion paper Wintjen et al., 2022). The aim of this measurement campaign covering the time frame from January 2016 to June 2018 was to quantify background concentration and deposition levels as well as their temporal dynamics for further improvements in modeling nitrogen deposition that may be used for further defining environmental protection guidelines. Therefore, we present modeled concentrations, deposition velocities, and fluxes of ΣN_r and compare them to measurements of the same variables (1), discuss the influence of micrometeorological parameters on modeled deposition velocities of ΣN_r and the impact of measured and modeled input parameters on modeled NH_3 fluxes (2), and compare annual N_r budgets of LOTOS-EUROS with DEPAC-1D, flux measurements, and nitrogen deposition estimates based on CBT reviewing them in the context of critical loads (3).

2 Materials and Methods

2.1 Site and campaign description

The campaign took place at a remote location in the Bavarian Forest National Park (NPBW) (48° 56'N 13°25'E, 807 m a.s.l.), a natural mixed forest located close to the Czech Border in the southeast of Germany. Due to the absence of nearby anthropogenic emission hotspots in terms of intensive agriculture or industry, concentrations of air pollutants are at background concentration level (Beudert and Breit, 2010). Observations of air pollutants and micrometeorology started on a 50 m tower in the 1980s. The measurement site is located in the Forellenbach catchment (Beudert and Gietl, 2015). The Forellenbach site is part of several networks for monitoring air pollution, e.g., International Cooperative Program on Integrated Monitoring of Air pollution Effects on Ecosystems (ICP IM) within the framework of the Geneva Convention on Long-Range Transboundary Air Pollution (UNECE, 2022) and Long Term Ecological Research (LTER, 2022). The Federal Environment Agency (UBA) and the NPBW Administration are responsible for the contribution to these networks. Further details about the site can be found in Zöll et al. (2019) and Wintjen et al. (2022).

For the application of DEPAC-1D, time series of micrometeorological parameters (i.e. temperature, atmospheric pressure, relative humidity, global radiation, Obukhov length, friction velocity) and air pollutant concentrations (NO, NO_2, HNO_3, NH_3, NO_3^-, NH_4^+, and sulphur dioxide (SO_2)) are required for the flux calculations. These concentration measurements were performed using a DELTA (DEnuder for Long-Term Atmospheric sampling e.g., Sutton et al., 2001; Tang et al., 2009) system

installed at 30 m above the forest floor. NH₃ was additionally collected by passive samplers of the IVL type (Ferm, 1991) at several levels from the ground to 50 m including 30 m. In addition, high resolution measurements of NH₃ were made with a Quantum Cascade Laser (QCL) (model mini QC-TILDAS-76 from Aerodyne Research, Inc. (ARI, Billerica, MA, USA)). The

125   setup was completed by the TRANC integrated in an EC system consisting of a sonic anemometer (GILL-R3, Gill Instruments, Lymington, UK) and a chemiluminescence detector (CLD 780 TR, ECO PHYSICS AG, Dürnten, Switzerland). This system allowed flux measurements of ΣN_r and common micrometeorological parameters. All instruments were installed at 30 m except for the CLD, which was placed in an air-conditioned box at the ground and connected to the TRANC via a 45 m opaque PTFE sampling line. NO, NO₂, and further meteorological parameters including pressure and global radiation were observed by the

130   NPBW at 50 m. Profile measurements of relative humidity and temperature were made at 10 m, 20 m, 40 m, and 50 m height. All devices installed at the site as well as the TRANC are described in Wintjen et al. (2022).

2.2 Modeling reactive nitrogen fluxes

2.2.1 Bidirectional resistance model DEPAC

135   In surface-atmosphere exchange models, fluxes are calculated by using resistance schemes. In case of gases exhibiting bidirectional exchange behavior, the flux F is defined as follows

$$F = -v_\mathrm{d}(z-d) \cdot (\chi_\mathrm{a}(z-d) - \chi_\mathrm{tot}) \tag{1}$$

The flux is a product of the deposition velocity (v_d) with the concentration difference between the atmospheric concentration and the compensation point of the trace gas χ_a. Both, the dry deposition or exchange velocity as the atmospheric concentration, are height dependent and given for an aerodynamic reference height $z-d$ where z is the geometric height and d the zero-plane

140   displacement height. The following convention is used for the fluxes: negative values represent deposition, positive values emission. Following the conductivity-resistance analogy, v_d is the inverse of the sum of the aerodynamic resistance (R_a), the quasi-laminar resistance (R_b), and the canopy resistance (R_c).

$$v_\mathrm{d} = (R_\mathrm{a} + R_\mathrm{b} + R_\mathrm{c})^{-1} \tag{2}$$

DEPAC (van Zanten, et al., 2010) can be used to calculate the dry deposition of reactive nitrogen gases. The aerodynamic (R_a) and laminar layer (R_b) resistances are required by DEPAC as input variables. Hence, the module is oriented at determining

145   R_c for NO, NO₂, HNO₃, and NH₃. R_c is treated differently for each N_r compound but basically as the sum of parallel resistances, which model the exchange behavior of the atmosphere and vegetation:

$$R_\mathrm{c}^{-1} = R_\mathrm{w}^{-1} + R_\mathrm{stom}^{-1} + (R_\mathrm{inc} + R_\mathrm{soil})^{-1} \tag{3}$$

The stomatal resistance (R_stom) is calculated following Emberson et al. (2000a, b). In this scheme, stomatal conductance is determined by vegetation type dependent on maximum conductance lowered by factors controlling stomatal opening, i.e. light

150   intensity, ambient temperature, vapor pressure deficit, and soil water content, using well known Jarvis functions (Jarvis, 1976). For NH₃ a stomatal compensation point (χ_stom) is calculated following Wichink Kruit et al. (2010, 2017). The cuticular resistance (R_w) is described by Sutton and Fowler (1993) for NH₃ and the corresponding cuticular compensation point based on the works of Wichink Kruit et al. (2010, 2017). For NO and NO₂, R_w is set considerably high to 10000 and 2000 s m⁻¹, respectively, allowing hardly any deposition on external surfaces. The in-canopy resistance (R_inc) is given by van Pul and

155   Jacobs (1994), and the soil resistance (R_soil) is described following Erisman and van Pul (1994). In the current version of

DEPAC, the soil compensation point is set to zero for all surface types. In case of HNO₃, a fast uptake to any surface is assumed through a low, constant R_c of 10 s m⁻¹. The total compensation point is determined as written in van Zanten et al. (2010).

$$\chi_{\text{tot}} = \frac{R_c}{R_w} \cdot \chi_w + \frac{R_c}{R_{\text{inc}} + R_{\text{soil}}} \cdot \chi_{\text{soil}} + \frac{R_c}{R_{\text{stom}}} \cdot \chi_{\text{stom}} \tag{4}$$

For further details to the documentation of DEPAC, we refer to the publication of van Zanten et al. (2010). Following implementation in LOTOS-EUROS, the version of DEPAC used in this study differs from the one documented in van Zanten et al. (2010) in two main aspects: Firstly, the implementation of a function considering co-deposition of SO₂ and NH₃ (Wichink Kruit et al., 2017) in the non-stomatal pathway and secondly, the usage of a monthly moving NH₃ average concentration for determining the stomatal compensation point (Wichink Kruit et al., 2017).

2.2.2 Modeling of ΣNᵣ deposition (LOTOS-EUROS)

LOTOS-EUROS (Manders et al., 2017) simulations were performed for the entire measurement period. For this purpose, a large-scale simulation was setup for Europe in which a second domain covering northwestern Europe at 7x7 km² was nested. The simulations were forced with weather data from the European Centre for Medium range Weather Forecast (ECMWF) and the CORINE-2012 land-use classification. For the European background simulation, the CAMS-REG European emission inventory (Kuenen et al., 2021) was used. For the inner domain the emission data for Germany were replaced by the national emission inventory. Modeled concentrations were written out for a reference height of 2.5 m. The land use specific and total dry deposition were calculated by LOTOS-EUROS on hourly basis for NH₃, NO, NO₂, HNO₃, NO₃⁻, and NH₄⁺. Dry deposition of particles was calculated according to Zhang et al. (2001) (see Manders-Groot et al. (2016, Sec. 5.2)). The Corine Land Cover 2012 classification of the grid cell, in which the measurement site was located, was divided into 46.0 % seminatural vegetation, 37.2 % coniferous forest, 15.9 % deciduous forest, 0.7 % water bodies, and 0.2 % grassland. However, the actual structure of the forest stand showed 81.1 % coniferous forest and 18.9 % deciduous forest within the footprint of the flux measurements during the measurement campaign. Due to differences in the distribution of vegetation types in the footprint, results from LOTOS-EUROS were calculated with the site-specific weighting of land-use classes of the flux tower's footprint. The low contribution of coniferous forest and deciduous forest within the grid cell may be related to the evaluation of older aerial photographs showing larger areas of deadwood. Finally, the dry deposition of ΣNᵣ was calculated as the sum of the individual Nᵣ fluxes. A detailed documentation of LOTOS-EUROS is given in Manders-Groot et al. (2016) and Manders et al. (2017).

2.2.3 Site-based modeling of ΣNᵣ deposition (DEPAC-1D)

DEPAC-1D is a stand-alone version of LOTOS-EUROS' dry deposition module DEPAC using a FORTRAN90 wrapper program to accept arbitrary input datasets. DEPAC-1D used micrometeorological variables and parameters measured at the site to estimate R_c and the compensation point of NH₃. The atmospheric resistances – R_a and R_b – and the fluxes of NH₃, NO, NO₂, HNO₃, NO₃⁻, and NH₄⁺ were calculated outside DEPAC following Garland (1977) and Jensen and Hummelshøj (1995, 1997) with stability corrections after Webb (1970) and Paulson (1970). The deposition of particles was calculated following Zhang et al. (2001) (see also Manders-Groot et al. (2016, Sec. 5.2)) and therewith equal to LOTOS-EUROS. Note that particle deposition is strictly speaking not part of the DEPAC module and was modeled with a separate program implementing the particle deposition scheme used within LOTOS-EUROS.

For estimating fluxes with DEPAC-1D, concentration measurements on monthly and half-hourly basis were used. NH₃ fluxes were mostly based on half-hourly concentration measurements of the NH₃ QCL. Half-hourly gaps in the NH₃ concentration time series were assigned with their monthly integrated concentration value obtained from DELTA samplers. If these measurements were not available, missing values were replaced by monthly integrated results from passive sampler

195 measurements of NH₃. During winter, the uncertainty introduced by this gap-filling approach seems to be low as suggested by
Schrader et al. (2018). We did not superimpose gap-filled concentration values with a diurnal pattern or used monthly averages
of half-hours to fill gaps in concentration time series, since instationarites in the NH₃ concentration pattern could not be
reproduced by a synthetic diurnal cycle or monthly averages of half-hourly values. Fluxes of HNO₃, NO₃⁻, and NH₄⁺ solely
based on monthly DELTA measurements. Gaps in time series of these compounds and SO₂ were replaced by monthly averages

200 from adjacent years. NO and NO₂ fluxes were based on half-hourly measurements routinely taken at 50 m. The difference in
measuring height was considered in the calculation of R_a. SO₂ and NH₃ concentrations from gap-filled DELTA time series
were used to determine compensation points and additional deposition corrections, similar to the use of monthly averages
when using DEPAC within LOTOS-EUROS.

205 All micrometeorological parameters were available at half-hourly resolution. Temperature and relative humidity data
corresponded to the average of measurements from 20 m and 40 m height above ground. Since profile measurements of
temperature and relative humidity started in April 2016 (Wintjen et al., 2022), measurements at 50 m were used until end of
March 2016. Pressure and global radiation measurements were taken at 50 m, too. Indicators of stability and turbulence such
as the Obukov length and friction velocity were obtained from momentum flux measurements of the sonic anemometer. For

210 modeling R_a, the solar zenith angle, which is calculated by using celestial mechanic equations, the roughness length (z_0), and
d are needed. We set z_0 to 2.0 m and d to 12.933 for coniferous forest and to 11.60 m for deciduous forest, corresponding to
LOTOS-EUROS defaults for these land-use classes. Leaf area index (LAI) was modeled as described by van Zanten et al.
(2010). The LAI determined from the site-specific land-use class weighting ranged between 4.1 and 4.8.

215 The calculation of the dry deposition was made for NH₃, NO, NO₂, HNO₃, NO₃⁻, and NH₄⁺ with the mentioned input data on
half-hourly basis. Results from DEPAC-1D were weighted with the site-specific land-use distribution within the flux
measurement's footprint (81.1 % coniferous forest and 18.9 % deciduous forest). We compared them to dry deposition fluxes
of LOTOS-EUROS as well as the measured ΣNᵣ fluxes estimated with the EC method from TRANC measurements (Wintjen,
et al. 2022). In order to compare the results from modeling to TRANC measurements, we filled gaps in the TRANC flux data

220 given by Wintjen et al. (2022) with results from DEPAC-1D. Those gaps were related to insufficient turbulence mostly
occurring during nighttime, performance issues of the instruments, etc. Gaps in DEPAC-1D were mostly related to power
outages causing gaps in micrometeorological data and issues in the measurements of Nᵣ compounds. Respective half-hourly
values in the flux time series of each gas (approx. 3.4% for NH₃, HNO₃, NH₄⁺, and NO₃⁻ and 9.3% for NO and NO₂) were filled
with results from LOTOS-EUROS. We further made a combination of Mean-Diurnal-Variation (MDV) approach (Falge et al.,

225 2001) and DEPAC-1D. Analogous to Wintjen et al. (2022), MDV was applied to short-term gaps (less than 3 days), but instead
of using monthly diurnal averages of specific half-hours to replace missing values in long-term gaps we used DEPAC-1D. The
window for filling a gap with MDV was set to ±5 days, gaps spanning time frames of more than 3 days were treated as long-
term. Both approaches, DEPAC-1D alone and the combination of DEPAC-1D and MDV, were able to fill all gaps in flux
time series. Uncertainties of the gap-filled fluxes determined by MDV were calculated as the standard error of the mean.

230 Cumulative uncertainties of TRANC fluxes solely based on the uncertainty of the gap-filling and were calculated according to
Eq. (3) of Wintjen et al. (2022). The error calculation scheme proposed by Brümmer et al. (2022) (Eq. (1)) was applied to
fluxes filled with DEPAC-1D. Flux uncertainty of those half-hours was given as

$$F_{\text{unc,DEPAC-1D}} = \frac{\tilde{X}}{F_{\text{DEPAC-1D}}} \; ; \; with \; \tilde{X} = \frac{F_{\text{unc,meas}}}{F_{\text{meas}}} \qquad \textbf{(5)}$$

where $\tilde{X}$ represents the median of the ratio of the uncertainty of the measured fluxes ($F_{\text{unc,meas}}$) to their corresponding flux
values (F_{meas}). The uncertainty of the measured fluxes was given by Finkelstein and Sims (2001). Systematic uncertainties

235 were not accounted in the error calculation. A discussion on systematic uncertainties is given in Wintjen et al. (2022).

2.3 Measuring nitrogen outflow from the canopy using the Canopy Budget technique (CBT)

The canopy budget technique (CBT) is the most common method for estimating total and dry nitrogen deposition in
240 ecological field research based on inorganic nitrogen fluxes (NO_3^- , NH_4^+) only (see Staelens et al., 2008, Table 1). Total
deposition of dissolved inorganic nitrogen (DIN_t) was estimated on yearly basis after the CBT approach of Draaijers and
Erisman (1995) and de Vries et al. (2003) whose results differed only marginally and were therefore averaged. The
biological conversion of deposited inorganic nitrogen into dissolved organic nitrogen (DON) in the canopy, which is not
addressed in CBT was estimated by the difference of DON fluxes between throughfall and bulk deposition (ΔDON). Adding
245 ΔDON to throughfall DIN or to DIN_t reveals a frame of lower and upper estimates of total nitrogen deposition (N_t) and, by
subtracting DIN deposition at an open land site from these N_t, of lower and upper estimates of dry deposition (Beudert and
Breit, 2014).

3 Results

3.1 Comparison of modeled and measured concentrations

250 Figure 1 shows the modeled concentrations of LOTOS-EUROS for each N_r compound and their sum in comparison to the
TRANC measurements. Looking at concentrations and patterns of each of the individually modeled compounds, reveals that
NH_3 had the highest concentrations, in particular in spring and partially in autumn with values close to zero in winter. On
average, LOTOS-EUROS predicted an average NH_3 concentration of 1.8 µg N m^{-3}. During spring, modeled concentrations
exceeded 10 µg N m^{-3}. Such high concentration levels were not reached by the other N_r compounds. In winter, NO_2
255 concentrations reached up to 5 µg N m^{-3}, whereas concentrations were negligibly small in summer. The concentrations of NO
and HNO_3 were close to zero during the entire measurement campaign. Only during summer HNO_3, showed slight variations.
Average concentrations of NO_3^- and NH_4^+ were similar to NO_2. Particle concentrations were lowest in summer and reached
values up to 5 µg N m^{-3} in spring. The comparison of measured and modeled ΣN_r revealed significant discrepancies in
concentration values. Except for the summer, modeled half-hourly concentrations were two to three times higher than the
260 measured values. Average ΣN_r concentration modeled with LOTOS-EUROS was 5.0 µg N m^{-3}, whereas the average measured
concentration with the TRANC was 3.1 µg N m^{-3}. The discrepancy being largest during spring clearly corelates with the
modeled ammonia concentrations.
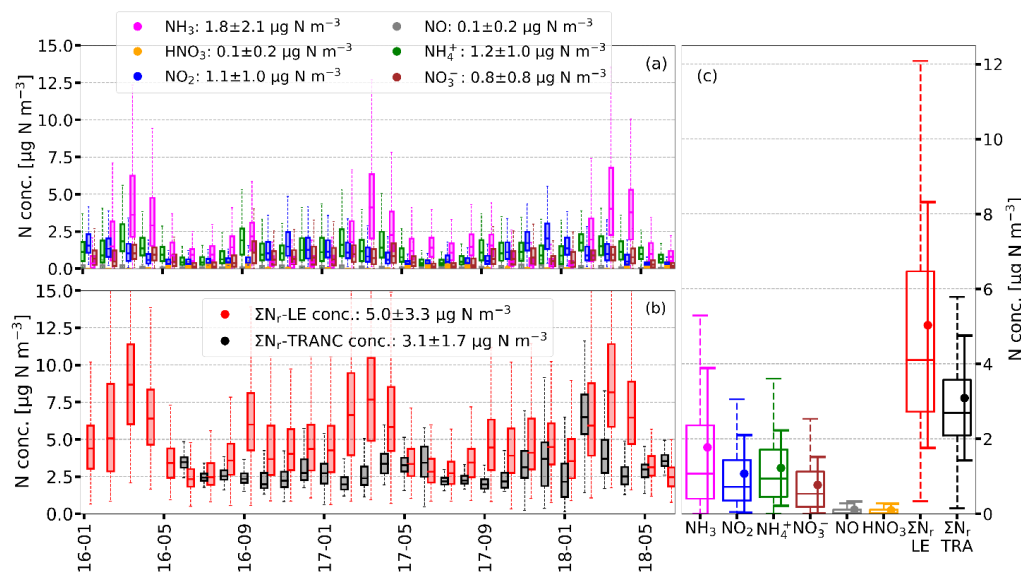
Figure 1. Concentrations of NH$_3$ (fuchsia), NO$_2$ (blue), NO (grey), HNO$_3$ (orange), NH$_4^+$ (green), NO$_3^-$ (brown), and their corresponding
265   sum (red) predicted by LOTOS-EUROS (LE) compared to ΣN$_r$ (black) obtained from TRANC measurements represented as box-and-
whisker plots (box frame = 25 % to 75 % interquartile range (IQR), bold line = median, whisker = 1.5*IQR)) on monthly basis ((a) and (b))
and for the entire duration of the campaign (January 2016 to end of June 2018) (c) in µg N m^{-3}. In the legends, averages and standard
deviations referring to the entire campaign for ΣN$_r$ and its individual compounds are shown.

The large modeled NH$_3$ concentrations by LOTOS-EUROS could not be verified by the observed levels of the passive

270   samplers, the DELTA system, and the QCL. Figure S1 shows a comparison of these measurement techniques with NH$_3$

concentrations predicted by LOTOS-EUROS. A two- to threefold overestimation of NH$_3$ concentrations by LOTOS-EUROS

is visible. In addition, the modeled seasonal pattern was not in agreement with the measurements, for example, the increase in

NH$_3$ during autumn was not observed by the instruments.

A comparison of the individual measured N$_r$ compounds by DELTA to LOTOS-EUROS is displayed in Fig. 2. The discrepancy

275   in the seasonal pattern of NH$_3$ is obvious. The distinct peaks occurring in February, March, April, September, and October

were not found by DELTA. ΣN$_r$ values of DELTA and TRANC showed a reasonable agreement and ΣN$_r$ concentrations

showed only small seasonal differences whereas LOTOS-EUROS overestimated ΣN$_r$ of the TRANC by ca. 2 µg N m^{-3}. The

high ΣN$_r$ concentrations of LOTOS-EUROS were mainly related to NH$_3$. In addition, NO$_3^-$ and NH$_4^+$ were not in agreement

with values determined by DELTA. Considering the entire campaign, median differences to DELTA were 0.57, 0.77, and 0.87

280   µg N m^{-3} for NH$_3$, NO$_3^-$, and NH$_4^+$, respectively (see Fig. S2). HNO$_3$ concentrations agreed well (0.08 µg N m^{-3}), and NO$_x$ was

slightly lower in the LOTOS-EUROS simulations (0.32 µg N m^{-3}) (Fig. S2).
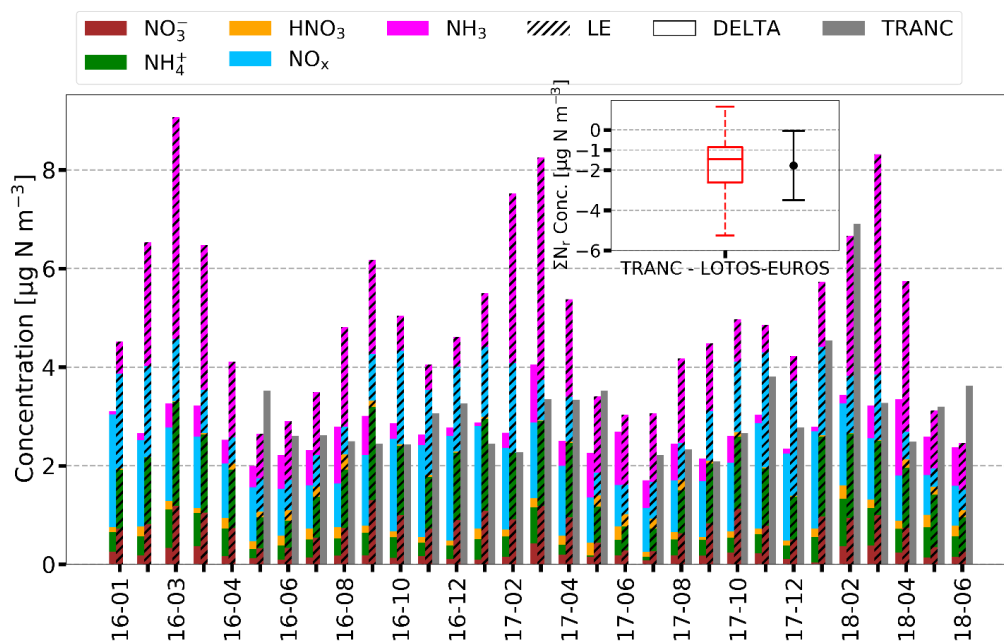
Figure 2. Monthly stacked concentration of LOTOS-EUROS (LE) (hatched), TRANC (grey), DELTA, and NO_x in µg N m^{-3} for the
285   entire measurement campaign. Gaps in the NH_3 timeseries caused by a low pump flow of the denuder pump were filled with passive
sampler values from 30 m. This procedure was done for December 2016 and 2017, March 2018, and April 2018. Remaining gaps in the
time series of HNO_3, NH_4^+, and NO_3^- were replaced by monthly averages estimated from other years if available. In case of NH_3, the
procedure was applied to January 2017. For the other compounds, the gap-filling was done for December 2017, March 2018, and April
2018. Results from LOTOS-EUROS, TRANC, and NO_x measurements were averaged to the exposure periods of the DELTA samplers. In
290   the small panel, the difference in the monthly ΣN_r concentrations of TRANC and LOTOS-EUROS is shown represented as box-whisker-
plot (box frame = 25 % to 75 % interquartile range (IQR), bold line = median, whisker = 1.5*IQR)) (red) and average with error bars
indicating the standard deviation (black) for the entire measurement campaign.

Since NH_3 contributed most to ΣN_r in LOTOS-EUROS, seasonal contributions of the N_r compounds were different to results

295   determined from DELTA and NO_x measurements. Wintjen et al. (2022) determined NO_x as predominant compound in the ΣN_r

concentrations. LOTOS-EUROS states the NH_3 as the most important compound contributing to ΣN_r as shown by Fig. S3. By

comparing Fig. S3 and Fig. 2, we examined that LOTOS-EUROS and DELTA found seasonal changes for NH_3 with the

highest contribution in spring and lowest in winter. However, the contribution of NH_3 to ΣN_r was surprisingly high (29 %)

compared to the observations (4.9 %) during winter. As expected from Fig. 2, HNO_3 contributions were comparable between

300   LOTOS-EUROS and DELTA. Particle contribution was higher in the model, and their contributions and concentrations were

invariant to seasonal changes except for spring.

3.2 Modeled N_r deposition velocities and fluxes of DEPAC-1D

The comparison of the deposition velocities and fluxes for each N_r compound modeled by DEPAC-1D is shown in Fig. S4 and

305   S5 displayed as monthly box-and-whisker plots, respectively. For the data description. medians were preferred to reduce the

influence of outliers on reported deposition velocities and fluxes.

In case of HNO_3, a median v_d of 1.56 cm s^{-1} was determined by DEPAC-1D. During the entire campaign, IQR and positions

of the whiskers showed less interseasonal variations with largest values of 4.27 cm s^{-1}. From May to September, the flux

median was -3.35 ng N m^{-2} s^{-1} whereas -2.04 ng N m^{-2} s^{-1} was determined for the other months. Largest fluxes were found for

310   May and June with values close to 10.0 ng N m^{-2} s^{-1} caused by slightly higher concentrations compared to the rest of the year.

Deposition velocities of NO_2 were close to zero in winter. From April to October, monthly median deposition velocities ranged between 0.07 and 0.35 cm s^{-1} with largest values (1.5*IQR; see Fig. S4) close to 1.0 cm s^{-1}. The seasonal pattern in v_d is transferable to the predicted fluxes. Fluxes were enlarged from April to October, but flux medians showed hardly any monthly variations, and flux median was at -1.57 ng N m^{-2} s^{-1}. Similar to HNO_3, largest fluxes (1.5*IQR; see Fig. S5) reached up to -

315   10.0 ng N m^{-2} s^{-1}. Modeled deposition velocities of and fluxes of NO were the lowest in DEPAC-1D and negligible compared to the other compounds

Only during winter, monthly median deposition velocities of NH_3 were close to zero. From March to August, deposition velocities were larger, and monthly medians ranged between 0.55 and 2.17 cm s^{-1} but extensions of the IQR and whiskers in the boxplots were similar (Fig. S4). Overall, the median NH_3 deposition was 7.87 ng N m^{-2} s^{-1} for DEPAC-1D. From the

320   seasonal point of view, hardly any deposition was predicted for winter, and a median deposition of 10.52 ng N m^{-2} s^{-1} was found during spring.

Monthly median deposition velocities of NO_3^- and NH_4^+ followed the same temporal pattern with lower values lowest in summer and higher in winter. During summer, monthly median deposition velocities were close to zero. Median v_d was 0.01 and 0.05 cm s^{-1} for NO_3^- and NH_4^+ during winter, respectively. Only in February 2018, whiskers of DEPAC-1D extended up

325   to 0.37 and 1.27 cm s^{-1} for NO_3^- and NH_4^+, respectively. For the entire campaign, DEPAC-1D monthly flux medians of NO_3^- and NH_4^+ were lower than -0.05 and -0.60 ng N m^{-2} s^{-1}. In February 2018, whiskers for DEPAC-1D extended to -11.0 and -1.0 ng N m^{-2} s^{-1} for NH_4^+ and NO_3^-, respectively (see Fig. S5).

A comparison of the modeled and measured v_d for the ΣN_r flux is provided in Fig. 3. The modeled total nitrogen dry deposition

330   velocities were obtained by dividing the modeled dry deposition flux for all compounds by the modeled total nitrogen concentrations in ambient air. Differences between the median modeled and measured v_d typically ranged between -0.3 and 1.0 cm s^{-1}. Especially during the summer months, an overestimation of the modeled values was observed for the DEPAC-1D results. The modeled median values and diurnal cycles for winter months were quite comparable to the measured values.

335
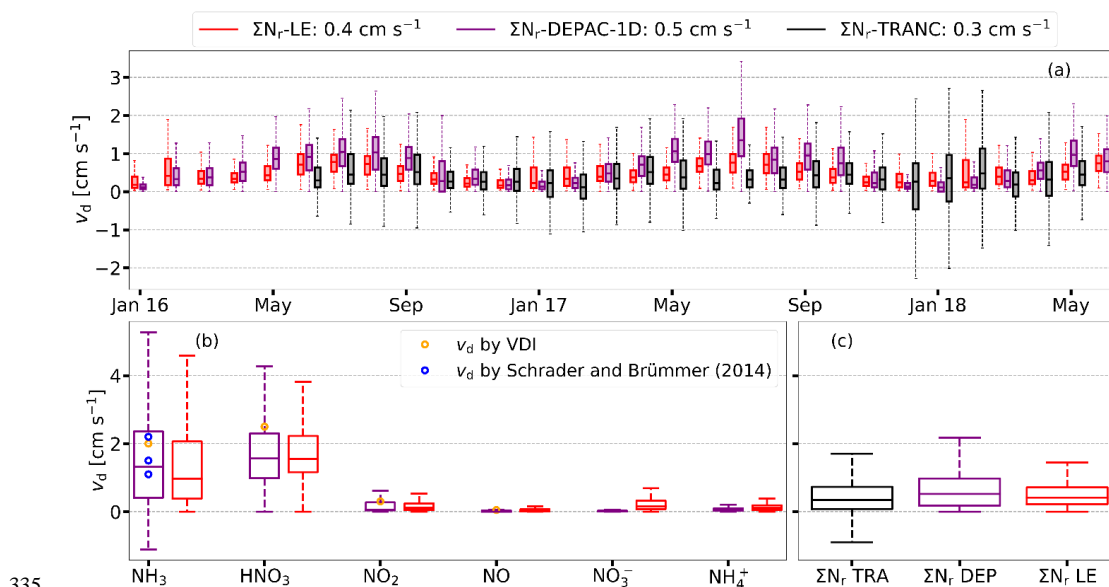
Figure 3. Monthly v_d of ΣN_r determined from TRANC (purple) measurements, DEPAC-1D (black), and LOTOS-EUROS (red) with the corrected land-use weighting in cm s^{-1} represented as box-and-whisker plots in the upper panel (a). In the corresponding legend median v_d related to the entire campaign are given. In the lower panels ((b) and (c)), box-and-whisker plots of v_d for each N_r compound and ΣN_r are shown based on the entire campaign (TRA=TRANC, DEP=DEPAC-1D, LE= LOTOS-EUROS). Blue circles are referring to NH_3 deposition
340   velocities reported by Schrader and Brümmer (2014) for deciduous forest, mixed forest, and spruce forest (from low to high), orange circles show deposition velocities proposed by VDI (2006).

As the DEPAC-1D was fed with measured concentration data, the comparison for the modeled ΣN_r fluxes shows a large degree of similarity to the results for the deposition velocity, see Fig. 6. The ΣN_r exchange of DEPAC-1D is close to zero during the

345   entire winter, and thus the difference to measured deposition was lowest during that time. During summer, a systematic overestimation of DEPAC-1D compared to measured fluxes was observed. Inspection of the diurnal cycles for May to September shows that both, the DEPAC-1D and measured data, exhibit a clear diurnal pattern with lowest deposition during the night and highest values around noon. However, where the measured data are close to zero during the night, the modeled flux show considerable nighttime fluxes. The latter may be due to the assumption of constant HNO_3 concentrations as input to

350   DEPAC-1D, whereas in reality the concentrations are low at night and maximize during the day. Note that improving this issue would result in an even larger overestimation of the flux during daytime.

To further examine the reasons behind these discrepancies, we show the diurnal cycles of v_d after classifying the ΣN_r deposition velocities for half-hours without precipitation during May-September in two groups being below or above the median temperature (T_{air} =14.6°C), relative humidity (RH = 74.0 %) and total ΣN_r concentration (c(ΣN_r) = 2.7 µg N m^{-3}). In addition,

355   we separated dry and wet leaf surfaces following the calculation scheme by Wintjen et al. (2022). The diurnal cycles illustrate the same diurnal biases as discussed above. Figure 4 shows that DEPAC-1D results indicate that lower temperatures, higher relative humidity, and wet leaf surfaces enhance the ΣN_r dry deposition velocity. This behavior was expected based on the models' parameterization, but it is in contradiction to the TRANC measurements. Especially, the differences for the relative humidity regimes are remarkable. Smaller differences are observed for the dependency on temperature and the ΣN_r

360   concentration, although both have a stronger influence in the model than on their measured counterpart.
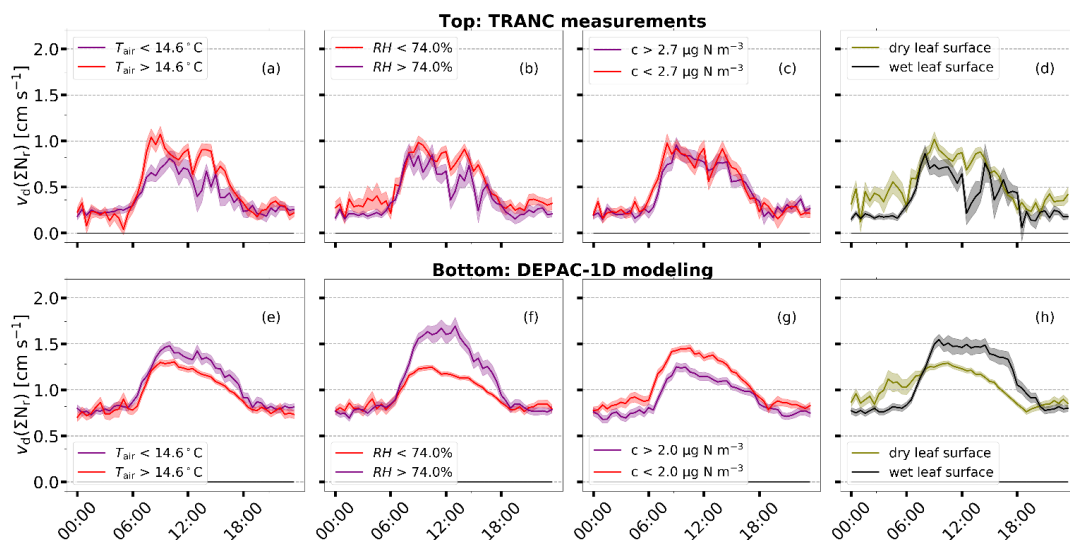
Figure 4. Averaged diurnal cycles of ΣN_r v_d for low and high temperature, relative humidity, concentration during the time frame May to September. The top row refers to TRANC measurements ((a) to (d)), the bottom row refers to DEPAC-1D modeling ((e) to (h)). Data was stratified after their median calculated for the entire period. Dry and wet leaf surfaces (Panel (d) and (h)) were identified following the

365   calculation scheme of Wintjen et al. (2022). Shaded areas represent the standard error of the mean.

3.3 Modeled N_r deposition velocities and fluxes of LOTOS-EUROS

Inspection of the dry deposition velocity for HNO_3 as calculated by LOTOS-EUROS (Fig. S4) showed a striking feature with unrealistically high values modeled for November 2017 to February 2018. Monthly median deposition velocities of LOTOS-

370   EUROS were higher than 1.90 cm s^{-1} and values of more than 10 cm s^{-1} were reached. As v_d depends mostly on the aerodynamic
       resistance, a maximum is expected during summer and normally present. The periods with high v_d in winter are characterized
       by snow cover. An error in the stability parametrization was found and will be corrected for after this study. The high v_d values
       during snow cover were present for all components for which subsequent resistances are small as well, i.e. HNO$_3$, NH$_3$, and
       nitrogen aerosols. The impact is also visible in the total nitrogen flux estimates, although not for all compounds. For example,

375   the HNO$_3$ flux in winter is near to zero as nitric acid is almost not present. Also, for NH$_3$ the impact is small. The main impact
       is through the deposition of NO$_3^-$ and NH$_4^+$ particles, which we will later correct for.

       The deposition velocities of NH$_3$ of LOTOS-EUROS showed a seasonal pattern comparable to DEPAC-1D but deviations in
       absolute values were found. From April to August, we determined monthly medians ranging from 0.43 to 1.76 cm s^{-1}. Except

380   for autumn, deposition velocities covered a wider range compared to DEPAC-1D. During that season, large values of up to
       10.0 cm s^{-1} were reached. Differences in v_d of NO$_2$ to DEPAC-1D were negligible. From April to October, monthly median
       deposition velocities of LOTOS-EUROS were between 0.11 and 0.30 cm s^{-1} and close to zero in winter. Analogous to DEPAC-
       1D, deposition of NO did not play a role in the LOTOS-EUROS modeling. Deposition velocities of aerosol NO$_3^-$ and NH$_4^+$
       exhibited the same seasonal pattern. We determined a median v_d of 0.11 cm s^{-1} for NH$_4^+$ and 0.15 cm s^{-1} for NO$_3^-$.

385

       From October to April, deposition fluxes of HNO$_3$ were nearly zero in LOTOS-EUROS but enlarged from May to September
       with a flux median of -1.56 ng N m^{-2} s^{-1} and maximum values close to 10.0 ng N m^{-2} s^{-1} (Fig. S5). Still, LOTOS-EUROS fluxes
       were generally lower than DEPAC-1D as represented by their monthly flux medians.
       In case of NH$_3$, a median deposition of 10.44 ng N m^{-2} s^{-1} was predicted by LOTOS-EUROS. Compared to DEPAC-1D,

390   LOTOS-EUROS monthly flux medians differed from zero during winter and extreme values in the order of 15.0 ng N m^{-2} s^{-1}
       were written out. Outside the snow-covered period, large discrepancies were recorded in February, March, and April. Medians
       of LOTOS-EUROS were higher by about 7.30 ng N m^{-2} s^{-1}. During spring, 14.58 ng N m^{-2} s^{-1} were modeled with LOTOS-
       EUROS as median deposition.
       In the LOTOS-EUROS simulations, NO$_2$ fluxes were generally lower and seasonal differences were less pronounced compared

395   to DEPAC-1D. From April to October, a median flux of -0.96 ng N m^{-2} s^{-1} was determined whereas -0.78 ng N m^{-2} s^{-1} was
       calculated during the rest of the year. During winter, median depositions of NO$_3^-$ and NH$_4^+$ were 1.40 and 1.76 ng N m^{-2} s^{-1},
       respectively, with values higher than 10.0 ng N m^{-2} s^{-1}. During the rest of the year, median depositions of NO$_3^-$ and NH$_4^+$ were
       approximately 0.65 and 0.78 ng N m^{-2} s^{-1}, respectively.

400   Overall, the modeled and measured total nitrogen dry deposition velocities of LOTOS-EUROS and TRANC showed a slightly
       better agreement compared to DEPAC-1D, but v_d of LOTOS-EUROS were still higher during summer and substantially high
       in winter due to the influence of NO$_3^-$ and NH$_4^+$ (see Fig. 3). Generally, deviations to the results of v_d for the ΣN$_r$ flux were
       related to the input data of LOTOS-EUROS. The disagreements to measured concentrations were elaborated in Sect. 3.1,
       especially for NH$_3$, but also for nitrogen aerosols (see Fig. 2 and S2) leading to discrepancies to TRANC fluxes in spring and

405   winter (Fig. 6).

       To further investigate the impacts of the input data used in the LOTOS-EUROS simulations, we made a comparison of the
       measured and modeled input parameters used for the dry deposition modeling of NH$_3$ in LOTOS-EUROS (Fig. S6). The
       agreement of temperature and global radiation in terms of their coefficient of determination R^2 was good. We found marginal

410   differences of approximately 1.5°C and -6.13 W m^{-2} to measured values on average. High R^2 values were determined, namely
       0.97 for temperature and 0.78 for global radiation. A slight difference was found for relative humidity during the first half of
       2016. However, modeled values were higher by only 2.4 % on average, and the R^2 was still 0.67. In case of u_*, we found a

systematic difference, and the seasonal pattern did not agree well resulting in a lower R^2 of 0.43 compared to the other micrometeorological parameters. Modeled values were higher by 0.09 m s^{-1}. In particular from November 2017 to February

415   2018, the difference between modeled and measured u_* values was enlarged due to the snow cover effect. An increase in u_* reduces turbulent resistances leading to large deposition velocities and fluxes for compounds like HNO_3, NO_3^-, and NH_4^+ which are not or hardly affected by R_c.

The largest discrepancy was found for NH_3 concentration as illustrated by Fig. 2 and S1 in detail. All of these parameters play an important role in the modeling of the NH_3 exchange. In order to determine the impact of these parameters on modeled NH_3

420   fluxes, we calculated NH_3 fluxes for the land-use class spruce forest with DEPAC-1D by replacing a certain input parameter by its measured counterpart while all other input data were from LOTOS-EUROS. Figure 5 illustrates the results of this comparison. Since modeled temperature and global radiation agreed well with their measured counterpart, deposition of NH_3 is only marginally reduced if measured values were used. Relative humidity led to an increase in deposition, but the effect is constrained to approximately 6 %. We found significant differences in u_*, but considering measured values in the flux

425   calculation leads only to a reduction of 10 %. As expected from the analysis of Fig. S6, NH_3 concentration had the largest impact on deposition. Using measured NH_3 concentration reduced the deposition substantially by 42 % compared to the modeled deposition. As indicated by the lower panel, the largest discrepancy in fluxes was observed for the concentration case.
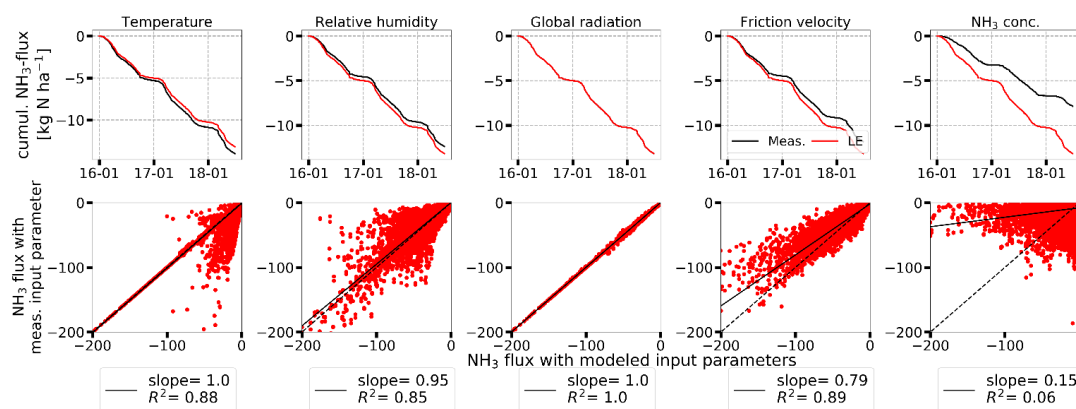
430   **Figure 5.** Comparison NH_3 fluxes calculated with DEPAC-1D for the land-use class spruce forest based on measured (black) and modeled input data (red). The comparison was made for temperature, relative humidity, global radiation, friction velocity, and NH_3 concentrations. In the first row, NH_3 fluxes are shown as cumulative sums in kg N ha^{-1}. In the second row, scatter plots of NH_3 fluxes in ng N m^{-2} s^{-1} are given. Linear regressions are shown as black, solid lines, black, dashed lines represent 1:1 lines.

3.4 Comparison of modeled and measured ΣN_r deposition fluxes

435   The comparison of modeled ΣN_r fluxes with TRANC fluxes is presented in Fig. 6. Only periods during which high quality flux measurements were available were considered for the analysis. Models were basically able to capture the seasonal pattern of the ΣN_r fluxes well, but generally overestimated the measured flux amplitude. The ΣN_r exchange of DEPAC-1D is near zero during the entire winter, and thus the difference to measured deposition was nearly zero. During summer, a systematic overestimation of DEPAC-1D to measured fluxes was observed. Modeled deposition of LOTOS-EUROS was slightly lower

440   than DEPAC-1D during summer and consequentially closer to measured fluxes. However, during autumn and spring predicted deposition of LOTOS-EUROS was significantly higher than deposition determined by DEPAC-1D and TRANC measurements due to the overestimated NH_3 concentrations. Similar observations were made during winter whereas median ΣN_r deposition of DEPAC-1D and TRANC was close to zero. Note that during February 2018 large aerosol concentrations were predicted and observed. The TRANC flux data also show the impact of the aerosol deposition, but to a larger extend as LOTOS-EUROS.
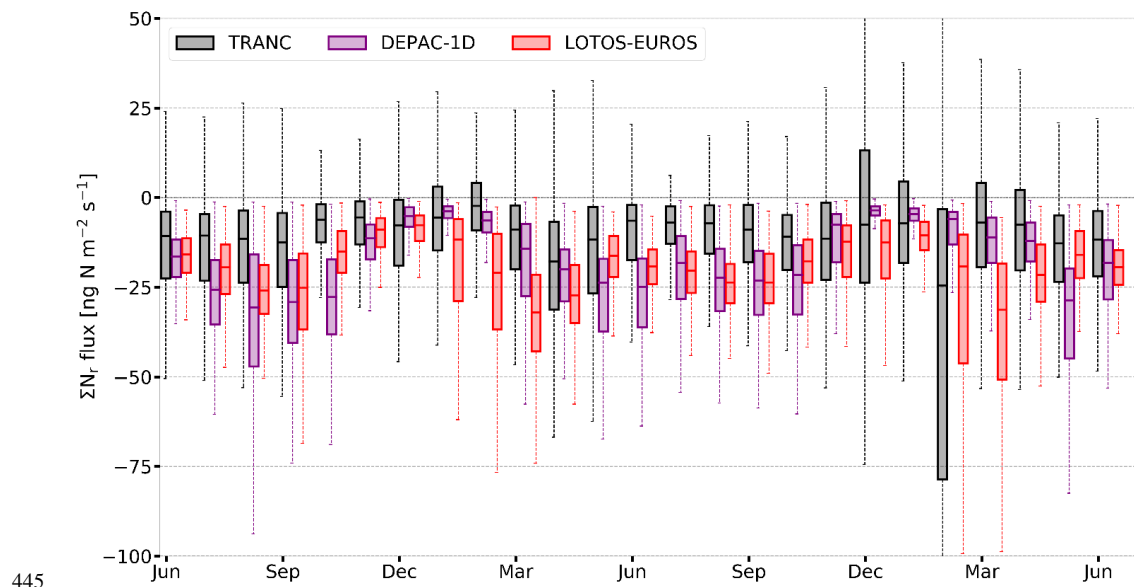
445

Figure 6. Fluxes of DEPAC-1D (purple), LOTOS-EUROS (red), and TRANC (black) from June 2016 to June 2018 shown as box-and-whisker plots. Whiskers of TRANC fluxes cover the range from -191 to 105 ng N m^{-2} s^{-1} in February 2018; the upper whisker of December 2017 reached 69 ng N m^{-2} s^{-1}.

Figure S7 shows exemplarily monthly diurnal cycles of ΣN_r based on TRANC, DEPAC-1D, and LOTOS-EUROS. As

450 previously written, during winter LOTOS-EUROS overestimated deposition whereas measurements showed near-zero exchange with emission phases. From May to September/October, DEPAC-1D exhibited a clear diurnal pattern with lowest deposition during the night and highest values around noon, which was in line with results from TRANC measurements. However, fluxes were systematically overestimated as indicated by Fig. 6 and Fig. S7 during those months. During the same period, ΣN_r deposition of LOTOS-EUROS was lower but still higher than TRANC fluxes except for September. During that

455 month, LOTOS-EUROS was similar to DEPAC-1D. Generally, the diurnal deposition pattern of LOTOS-EUROS did not agree well with DEPAC-1D and TRANC. Compared to DEPAC-1D and TRANC measurements, deposition showed fewer diurnal variations resulting in a smaller daily amplitude.

3.5 Cumulative N exchange and method comparison

To derive annual deposition numbers the gap-filling procedures were applied to the time series of the TRANC and DEPAC-

460 1D (see Sect. 2.2.3). Figure 7 shows the cumulative ΣN_r dry deposition of each method from January 2016 to end of June 2018. The contributions of the individual components to the dry ΣN_r deposition of DEPAC-1D were: 67.9 % NH$_3$, 15.3 % HNO$_3$, 10.4 % NO$_2$, 5.2 % NH$_4^+$, 1.0 % NO$_3^-$, and 0.1 % NO showing that modeled deposition was clearly driven by NH$_3$. Since emission processes could only be treated for NH$_3$, the observed emission of ΣN_r, for example deduced for December 2017 (Wintjen et al., 2022), could not be sufficiently modeled. Total compensation point (Eq. 4) was on average at 0.024 µg N m^{-3}.

465 Figure S8 shows the difference of ambient concentration and total compensation point for each month as boxplot. As seen by the whiskers, emission of NH$_3$ was possible only for certain periods in winter. Since NH$_3$ exchange was close to zero in winter, NH$_3$ emissions had hardly any influence on modeled total deposition of NH$_3$. The disagreement to TRANC deposition estimates was mainly related to the overestimation of ΣN_r fluxes in summer. Since the ΣN_r exchange was close to zero in winter, the difference to flux measurements was lower. As expected from the results above, LOTOS-EUROS exhibited a larger

470 discrepancy to flux measurements. Still, modeled ΣN_r deposition was lower than by using DEPAC-1D in summer, but in relation to flux measurements relatively high in winter and spring as indicated by the slope of their cumulative curves and in Fig. 6 and Fig. S7. Due to the snow cover effect, particle deposition was higher in LOTOS-EUROS, whereas gaseous

deposition   was   higher   in   DEPAC-1D.
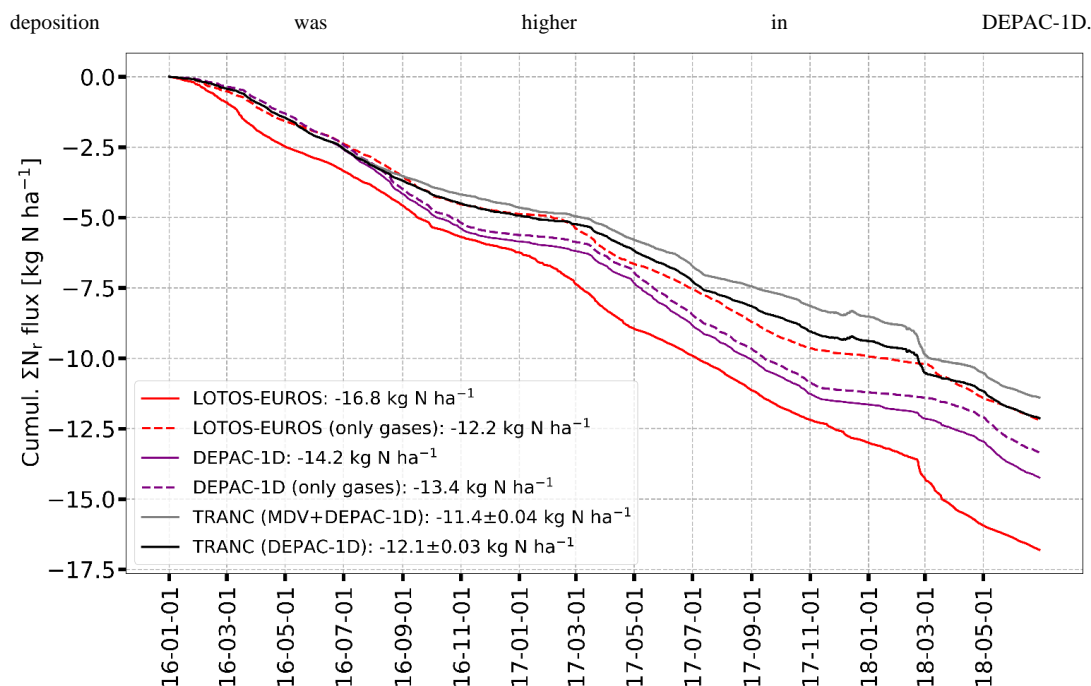
Figure 7. Comparison of measured and modeled cumulative ΣN_r dry deposition after gap-filling for the entire measurement campaign. Colors indicate different methods: TRANC+DEPAC-1D (black), TRANC+MDV+DEPAC-1D (grey), DEPAC-1D (purple), and LOTOS-EUROS (red). Dashed lines refer to cumulative dry deposition considering only gases. Number shown in the legend represent dry deposition and uncertainties after 2.5 years.

Both gap-filling strategies resulted in similar deposition estimates. After 2.5 years, the difference was estimated to be in the order of 700 g N ha^{-1}. Uncertainties related to gap-filling were negligible. Explicit differences in cumulative fluxes were found from June to September 2017 due to higher deposition fluxes in DEPAC-1D during those months. In February 2018, difference in measured deposition estimates was reduced since measured fluxes were larger than modeled fluxes of DEPAC-1D. Since all cumulative curves exhibit generally the same shape, we conclude that the variability in fluxes is reproduced by DEPAC-1D and LOTOS-EUROS well, although the amplitude and duration of certain deposition events is different. In Fig. 8, a comparison of the ΣN_r dry deposition separated by methods and measurement years is shown. Corresponding values of the dry deposition estimates are given in Table 1.

Table 1 ΣN_r dry deposition of TRANC, DEPAC-1D, LOTOS-EUROS, and CBT for the entire measurement campaign, i.e., January 2016 to June 2018. Results from CBT were weighted according to the measured land-use weighting. For a visualization of the annual dry deposition see Fig. 8.

Method	2016 [kg N ha^{-1} a^{-1}]	2017 [kg N ha^{-1} a^{-1}]	until June 2018 [kg N ha^{-1} a^{-1}]
TRANC (MDV+DEPAC-1D)	4.6	3.9	2.9
TRANC (DEPAC-1D)	4.9	4.5	2.7
DEPAC-1D	5.8	5.8	2.6
LOTOS-EUROS	6.2	6.8	3.8
CBT (lower estimate)	3.3	4.3	
CBT (upper estimate)	6.4	7.0	

In 2016, annual TRANC deposition was higher than in 2017. Using only DEPAC-1D as gap-filling technique, resulted in slightly higher dry deposition estimates. However, differences were negligible compared to their total dry deposition estimates.

495 Until June 2018, measured deposition was higher than the half of the previous years. DEPAC-1D deposition was nearly identical for 2016 and 2017, but lower than measured deposition until June 2018. The difference to TRANC estimates until June 2018 was caused by the deposition fluxes in February 2018, which had an influence on the MDV method leading to significantly larger gap-filled fluxes.

500 TRANC deposition was closer to the lower estimate of CBT, whereas DEPAC-1D predictions were within the standard deviation range of the CBT estimates. LOTOS-EUROS exhibited values close to the upper estimates of CBT. If we assume that the deposition from June to December 2018 would have been similar to the average of the previous measurement years (2.0, 2.3, 3.1, and 3.0 kg N ha^{-1} a^{-1} for TRANC (MDV+DEPAC-1D), TRANC (DEPAC-1D), DEPAC-1D, and LOTOS-EUROS, respectively), we would get dry deposition estimates similar to the previous years in case of TRANC and LOTOS-EUROS.

505 DEPAC-1D estimates would be lower than 2016 and 2017. Annual dry deposition estimated by CBT were close to each other for 2016 and 2017 and in the range of the long-term averages estimated from 2010 to 2018 (3.8 kg N ha^{-1} a^{-1} as lower estimate and 6.7 kg N ha^{-1} a^{-1} as upper estimate).

Averaging of the annual sums of each method for 2016 and 2017 resulted in a TRANC dry deposition of 4.3±0.4 and 4.7±0.2 kg N ha^{-1} a^{-1} depending on the gap-filling approach. DEPAC-1D showed 5.8±<0.1 kg N ha^{-1} a^{-1}, LOTOS-EUROS predicted

510 6.5±0.3 kg N ha^{-1} a^{-1}. We determined 6.7±0.3 kg N ha^{-1} a^{-1} with CBT as averaged upper estimate, and 3.8±0.5 kg N ha^{-1} a^{-1} as averaged lower estimate. It shows that dry deposition estimated by TRANC, DEPAC-1D, and LOTOS-EUROS were within the minimum and maximum deposition estimated by CBT but generally closer to the lower estimate of CBT except for LOTOS-EUROS.
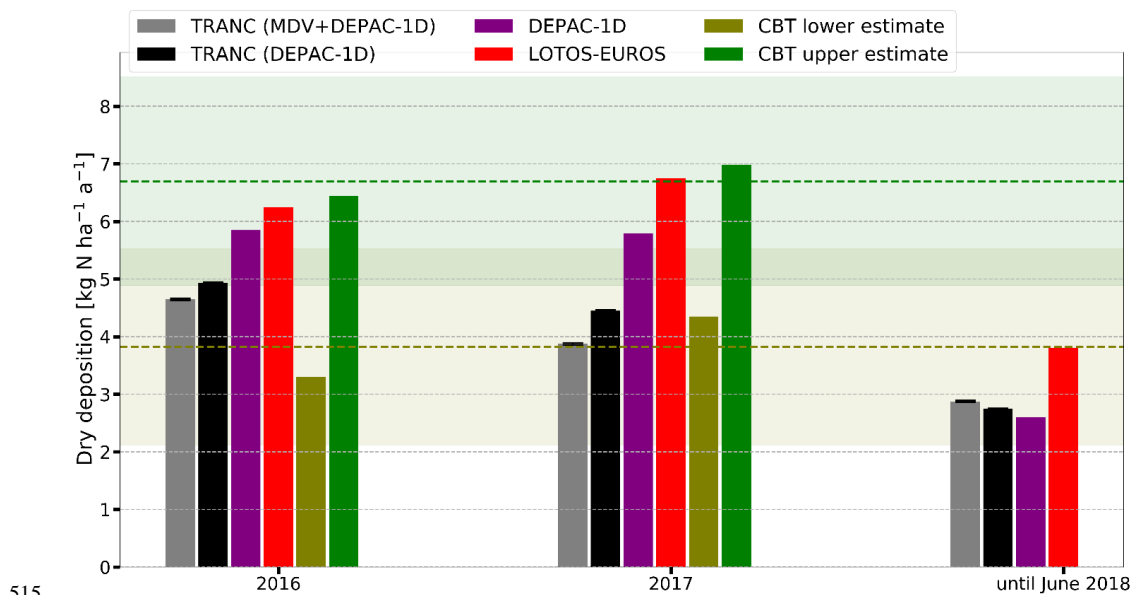
515

Figure 8. ΣN_r dry deposition for the years 2016 and 2017 and from January to June 2018 shown as bar chart. Colors indicate different methods: TRANC+DEPAC-1D (black), TRANC+MDV+DEPAC-1D (grey), DEPAC-1D (purple), LOTOS-EUROS (red), and canopy budget technique (olive and green). Data from TRANC, DEPAC-1D, and LOTOS-EUROS range from January 2016 to June 2018. CBTs' lower and upper estimates weighted according to the measured land use. The colored dashed lines indicate the averaged dry deposition of

520 the lower and upper estimates (dashed, brown line and dashed, olive line, respectively) were from 2010 to 2018, the shaded areas represent their standard deviation.

4 Discussion

4.1 Comparison of concentrations, fluxes, and annual budgets

525   The comparison to concentration measurements of NO, NO_2, and NH_3 conducted by Wintjen et al. (2022) revealed that NH_3 concentrations were systematically overestimated by LOTOS-EUROS during the entire campaign as described in Sec. 3.1 in detail. Modeled NO_x concentrations were similar or even lower than their measured values. Modeled seasonal patterns of NO_x and NH_3 agreed partly with their observed pendants. In case of NO_x, model and measurements reported highest values in winter and lowest values in summer mostly related to differences in emissions from enhanced heating and combustion

530   processes. In case of NH_3, a peak in the LOTOS-EUROS concentrations was found during spring. However, the predicted increase in NH_3 during autumn was not confirmed by the observations. Elevated NH_3 concentrations were most likely related to emissions from agriculture, in particular to the application of fertilizer during these times. Thus, the low pollution climate at the site could not be modeled well by LOTOS-EUROS.

Compared to other forest ecosystems, modeled concentrations of LOTOS-EUROS were closer to reported concentrations, e.g

535   for HNO_3 (Farmer et al., 2006; Horii et al., 2006; Farmer and Cohen, 2008), for NH_3 (Wyers and Erisman, 1998; Hansen et al., 2013,2015), for NO_3^- and NH_4^+ (Wolff et al., 2010; Gordon et al. 2011; Farmer et al. 2011, 2013), and NO_2 (Horii et al., 2004; Farmer and Cohen, 2006).

Modeled NH_3 fluxes were similar to observations of Hansen et al. (2015) ranging from -60 to 120 ng N m^{-2} s^{-1} above a

540   deciduous forest. The emission fluxes observed by Hansen et al. (2015) were probably caused by the decay of fallen leaves (Hansen et al., 2013) leading to less deposition during late summer and autumn compared to our site. During spring, Pryor et al. (2001) reported a daily deposition of 15 ng N m^{-2} s^{-1} for NH_3, which was comparable to predicted median depositions of DEPAC-1D and LOTOS-EUROS in the same season although ambient NH_3 concentrations were different. The high contribution of emission fluxes observed by Hansen et al. (2015) was not reproduced by the model applications at our site,

545   which was probably related to the negligible compensation point of NH_3. Since no compensation point is implemented for other N_r compounds, only deposition fluxes could be modeled for those compounds. In addition, their flux amplitude was significantly lower than for NH_3. Thus, the combined ΣN_r flux was mainly controlled by the NH_3 flux pattern.

Unlike NH_3, modeled NO fluxes had an insignificant contribution to the ΣN_r flux. Geddes and Murphy (2014) found that NO

550   fluxes were mostly downward with a maximum deposition of -2.9 ng N m^{-2} s^{-1} during daytime. The diurnal cycle of NO was reversed to NO_2 during the day and was nearly zero with a tendency of slight emission during the night (Horii et al., 2004; Geddes and Murphy, 2014). Thus, they observed emission of NO_2 during the day peaking at approximately 2.8 ng N m^{-2} s^{-1}. As a result, NO_x fluxes were slightly different from zero. Horii et al. (2004) found NO_2 deposition at concentrations higher than 1.1 μg N m^{-3} and emission fluxes in the opposite case. They further identified non-stomatal deposition as the strongest

555   contributor to the flux. Min et al. (2014) observed emission fluxes for NO and NO_2 during daytime but with even lower flux amplitude. Besides the emission fluxes, modeled deposition fluxes of NO_2 and NO were within the range of the reported values.

The contribution of NO to total modeled ΣN_r dry deposition was negligible due to the high canopy resistance implemented in

560   DEPAC. In general, NO is mainly observed as emission from soil if it is produced through (de)nitrification processes (Butterbach-Bahl et al., 1997; Rosenkranz et al., 2006). Most of the NO is rapidly converted to NO_2 in the presence of ozone (O_3) within the forest canopy, especially close to the ground (Rummel et al., 2002; Geddes and Murphy, 2014). Thus, NO fluxes were assumed to be close to zero in DEPAC at the reference height due to fast conversion processes within the forest

canopy and uptake possibilities like leaf surfaces for N_r compounds (e.g., Wyers and Erisman, 1998; Rummel et al., 2002;
565 Sparks et al., 2001; Gordon et al., 2011; Geddes and Murphy, 2014; Min et al., 2014; Wentworth et al., 2016).

It has to be considered that NO_2 is removed from the atmosphere by the reaction with O_3. During the night, NO_3 reacts with
NO_2 to dinitrogen pentoxide (N_2O_5). The latter can react with H_2O to HNO_3. HNO_3 as well as peroxyacetyl nitrates (PANs)
(Min et al. 2014) are effective sinks for NO_2, and HNO_3 has a significant impact on the measured deposition flux (Munger et
570 al., 1996). Modeled HNO_3 fluxes had a similar flux magnitude as the NO_2 fluxes. Comparing predicted HNO_3 fluxes with
values reported for different forest sites shows that HNO_3 was predominantly deposited at selected sites (see Walker et al.,
2020, Table 1) with values ranging from 1.4 to 40 ng N m^{-2} s^{-1} depending on forest types and time of the year. Modeled HNO_3
fluxes were at the lower end of published values.

575 Horii et al. (2006) reported inferred HNO_3 fluxes almost as high as the measured total NO_y fluxes. NO_y corresponds to the sum
of all oxidized nitrogen compounds, for example, NO, NO_2, particulate NO_3^-, HNO_3, N_2O_5, PAN, and other organic nitrates.
Their measured NO_y deposition ranged between 0 and 80 ng N m^{-2} s^{-1}. Comparing the values of NO_y and HNO_3 summarized
by Walker et al. (2020) shows that HNO_3 fluxes were almost as high as the NO_y fluxes highlighting their relevance in the NO_y
flux budget.

580
Modeled NO_3^- and NH_4^+ deposition fluxes were similar in magnitude and their absolute flux values were mostly below 1 ng
N m^{-2} s^{-1} considering their flux medians. NH_4^+ fluxes were similar to values reported by Farmer et al. (2011), who observed
NH_4^+ deposition with 1 ng N m^{-2} s^{-1} at maximum for a coniferous forest during midday. Gordon et al. (2011) found an average
NO_3^- flux of -0.8 ng N m^{-2} s^{-1} with a standard deviation of 1.5 ng N m^{-2} s^{-1}. Wolff et al. (2010) conducted measurements of
585 total ammonium (NH_3 and NH_4^+) and total nitrate (HNO_3 and NO_3^-) above a spruce forest. They determined mean fluxes of -
66 ng N m^{-2} s^{-1} and -41 ng N m^{-2} s^{-1} for tot-NH_4^+ and tot-NO_3^-, respectively. Modeled tot-NH_4^+ and tot-NO_3^- of LOTOS-
EUROS were significantly lower. Monthly medians ranged between -2.9 and -26.3 ng N m^{-2} s^{-1} and between -0.74 and -4.0 ng
N m^{-2} s^{-1} for tot-NH_4^+ and tot-NO_3^-, respectively. Similar values were calculated for DEPAC-1D.

590 In conclusion, modeled deposition fluxes are comparable to flux measurements conducted at various forest ecosystems.
However, comparison possibilities to flux measurements of N_r compounds, e.g., NH_3 and particles (Walker et al., 2020), above
forests are still sparse. In addition, most of the studies were carried out for a limited time of the year. The comparison revealed
that emission fluxes were observed for NH_3 and NO_2 due to the existence of a compensation point, the alternation of day and
night, or changes in surface properties or micrometeorology.

595
The comparison to TRANC fluxes indicated an overestimation of modeled ΣN_r. Predicted ΣN_r fluxes of DEPAC-1D were
systematically higher in summer, and LOTOS-EUROS ΣN_r deposition was suspiciously high in winter whereas measured and
site-based fluxes were close to zero. Median ΣN_r v_d of TRANC and LOTOS-EUROS were close to each other and lower than
DEPAC-1D for the entire campaign. Except for NH_3 and nitrogen aerosols, LOTOS-EUROS and DEPAC-1D gave similar
600 values for each compound (Fig. 3). In case of TRANC measurements, significant emission fluxes were found in winter as
discussed in Wintjen et al. (2022) for December 2017. Generally, emissions could not be sufficiently reproduced by the models
since emissions from soil are currently not included in DEPAC. The observed large deposition fluxes in February 2018 were
reproduced in the model simulations although the modeled flux amplitude was smaller. During that time, modeled
concentrations and fluxes of particulate N_r were the largest contributor to total ΣN_r, leading to the assumption of particle driven
605 ΣN_r deposition. DELTA measurements suggested that particulate NH_4^+ was most likely responsible for the measured ΣN_r
deposition (Wintjen et al., 2022). Modeled and measured NH_4^+ concentrations differed only by 0.75 µg N m^{-3} whereas a

significant disagreement was found between NH_3 measurements and LOTOS-EUROS (approx. 2.7 µg N m^{-3}). According to DELTA measurements, the NH_3 concentration was approximately 0.17 µg N m^{-3}. The averaged SO_2 concentration obtained from LOTOS-EUROS and DELTA were comparable during the exposure period of the samplers (1.5 and 2.0 µg m^{-3},

610 respectively). In case of the LOTOS-EUROS simulations, the dominant aerosol could have been NH_4NO_3 due to the high NH_3/SO_2 ratio (Trebs et al., 2005). In conclusion, the high deposition fluxes seem to be driven by particulate NH_4^+ compounds, ammonium sulfate and ammonium nitrate. DELTA measurements revealed a slightly lower concentration of the SO_4^{2-} than the NO_3^- aerosol, 1.28 and 1.63 µg m^{-3}, respectively, suggesting NH_4NO_3 as the aerosol likely responsible for the measured ΣN_r deposition. Still, the dominant aerosol is not fully known due to missing high-resolution measurements of nitrogen

615 aerosols.

The annual dry deposition estimates of all methods were in the same range considering uncertainties of measured fluxes and model applications (see Sect. 4.2 and 4.3). Annual estimates from TRANC were lower than the results from DEPAC-1D and LOTOS-EUROS. The reasons for the differences to the modeling approaches were elaborated in the previous sections. Possible

620 uncertainties regarding model applications are described in the subsequent sections. Uncertainties in TRANC measurements were discussed in Sect. 4.3 of Wintjen et al. (2022). At the measurement site, both gap-filling methods led to similar dry deposition estimates. During summer, we found differences in the gap-filled fluxes due to the systematic overestimation of DEPAC-1D. It should be kept in mind that NO_3^-, NH_4^+, and HNO_3 were measured by long-term samplers and monthly concentration estimates may not be fully representative of local events. Saylor et al. (2019) noted that v_d of particles for forest

625 are highly uncertain. Thus, differences to measurements could be expected. Besides missing emission fluxes in DEPAC-1D, the agreement of the dry deposition estimates was reasonable showing an inferential model like DEPAC-1D as an alternative gap-filling tool at sites or seasons with predominant N deposition.

Annual dry deposition estimates from TRANC, LOTOS-EUROS, and DEPAC-1D were found to be within the range of the lower and upper estimates of the CBT approach. Adding the wet-only deposition results reported in Wintjen et al. (2022) to

630 determined dry depositions, we calculated annual total depositions ranging between 11.5 and 14.8 kg N ha^{-1} a^{-1} noted in Table 2 for each year.

Table 2 Annual ΣN_r deposition of TRANC, DEPAC-1D, LOTOS-EUROS, and CBT for 2016, 2017, and from January to June 2018 in kg N ha^{-1} a^{-1}. Wet-only depositions of NO_3^-, NH_4^+, and DON were adapted from Wintjen et al. (2022).

Method	2016 [kg N ha^{-1} a^{-1}]	2017 [kg N ha^{-1} a^{-1}]	Until June 2018 [kg N ha^{-1} a^{-1}]
TRANC (MDV+DEPAC-1D)	12.9	11.7	6.3
TRANC (DEPAC-1D)	13.1	12.3	6.2
DEPAC-1D	14.1	13.6	6.1
LOTOS-EUROS	14.4	14.6	7.3
CBT (upper estimate)	11.5	12.2	
CBT (lower estimate)	14.6	14.8	

635 Comparing the results obtained from the measurement site to results obtained for other forest ecosystems using a similar validation procedure is rather difficult due to a large temporal and spatial variability in N_r compounds contributing to ΣN_r. Additionally, micrometeorological measurements as carried out in this study require substantial effort in maintenance and processing of the acquired data. Thus, most currently available EC measurements are limited to time periods covering a few weeks or months and are only available for certain locations.

640

Recently, Ahrends et al. (2020) compared deposition estimates of a CBT approach, an inferential method, and LOTOS-EUROS for several forest ecosystems. However, their CBT based on the variant suggested by Ulrich (1994), which is different to the

version used in this study, and their inferential method (IFM) was only applied to NO_2 and NH_3 due to the limited availability of ambient concentration measurements for other N_r compounds. In addition, deposition velocities for NO_2 and NH_3 were

645 calculated based on literature research for different forest types accompanied by various correction factors. They reported similar annual dry deposition estimates for CBT and IFM, which were found to be 12.6 and 12.9 kg N ha^{-1} a^{-1}, respectively. Minimum deposition was 3.8 kg N ha^{-1} a^{-1} for CBT and 1.0 kg N ha^{-1} a^{-1} for IFM. The lowest average deposition was 9.3 kg N ha^{-1} a^{-1} given by LOTOS-EUROS but minimum deposition was highest 6.3 kg N ha^{-1} a^{-1}. Since we measured N deposition in a low-polluted environment, the agreement to the minimum deposition estimates of Ahrends et al. (2020) seems reasonable.

650

In the consideration of critical loads, total nitrogen deposition is close to the proposed limits. Critical loads ranging from 10 to 15 kg N ha^{-1} a^{-1} and 10 to 20 kg N ha^{-1} a^{-1} were defined by Bobbink and Hettelingh (2011) for *Picea abies* and *Fagus sylvatica*, respectively. Since *Picea abies* was the prevailing tree species in the flux footprint (approx. 80%), the critical load of the investigated forest ecosystem is probably closer to the limits of *Picea abies*. Thus, the investigated forest ecosystem is in a

655 potentially endangered state. It should be kept in mind that this result refers to the current climatic situation and concentration level of various N_r compounds. Additionally, nitrogen input to the atmosphere on a broader scale will probably increase due to a growing population for which food security needs to be ensured. However, if proposed mitigation strategies on air pollutants, e.g., O_3 and NO_2, are successfully implemented in Europe, reductions in these gases could be still achieved even if global temperatures will rise by 2°C (Watson et al., 2016). Recently, van Damme et al. (2021) found that atmospheric NH_3

660 concentrations increased on different continents considering the years 2008 to 2018. Exceedances of critical loads could be still possible for forest ecosystems even at remote locations in the future.

4.2 Uncertainties in DEPAC-1D

We identified wet leaf surfaces, high relative humidity, and lower temperatures as conditions enhancing ΣN_r deposition from

665 May to September. Wet conditions hold an important role in the deposition of NH_3 (Wentworth et al., 2016) and cuticular deposition was identified as a larger sink for NH_3 than stomatal deposition (Wyers and Erisman, 1998). However, the results from TRANC measurements highlighted higher temperatures, lower relative humidity, and dry leaf surfaces as important factors enhancing ΣN_r deposition (Wintjen et al., 2022). Wet conditions, likely enhancing cuticular deposition of NH_3, seemed to be most responsible for the ΣN_r deposition at the measurement site as suggested by the models. The contradiction in wet

670 and dry conditions lead to the assumption that the current implementation of the NH_3 exchange pathways in DEPAC was not fully suited for predicting NH_3 deposition correctly under all site characteristics and situations and needs further investigation. It should be kept in mind that we measured ΣN_r exchange at low-polluted, mixed forest site (Beudert and Breit, 2010; Wintjen et al., 2022). Sites with different micrometeorology, vegetation, and pollution climate may exhibit other parameters like surface wetness, canopy temperature, and ambient concentration responsible for the ΣN_r exchange as found by Milford et al. (2001).

675 Further comparisons to flux measurements of ΣN_r and NH_3 are needed to investigate the role of stomatal and cuticular deposition.

Schrader et al. (2016) discovered problems in the calculation of the cuticular NH_3 compensation point under high ambient NH_3 concentrations and high temperatures, for instance during summer. The current implementation of Wichink Kruit et al. (2010)

680 in DEPAC likely underestimates the cuticular compensation point at high temperatures. This issue is not solved yet and could not be verified for our measurement site due to generally low NH_3 concentrations and the implementation of monthly averaged NH_3 concentration instead of half-hourly values in the concentration time series of NH_3 to some extent. However, NH_3 concentration were rather low at the measurement site, and the cuticular emission potential was estimated from monthly averaged concentrations in LOTOS-EUROS and DEPAC-1D, instead of instantaneous values as in the original

685 parameterization of Wichink Kruit et al. (2010), likely somewhat alleviating the issue discussed in Schrader et al. (2016). Thus, this issue could be not the main reason for the difference to flux measurements at our site. Unfortunately, NH_3 flux calculation with the EC method was not possible at the measurement site. No distinct time lag was found during the entire measurement campaign. Presumably, variability in measured raw concentrations of NH_3 could not be adequality identified by the NH_3 QCL (Ferrara et al., 2021; Wintjen et al., 2022).

690

In case of HNO_3, a constantly, low R_c is assumed leading to a median v_d similar to NH_3 since median R_c of NH_3 was about 15 s m^{-1} for the entire campaign. In general, deposition velocities of NH_3, HNO_3, NO_2, and NO proposed by the Association of German Engineers (VDI, 2006) were generally larger than modeled medians (see Fig. 3). Deposition velocity of NH_3 was in the range of values reported by Schrader and Brümmer (2014) for mixed forests. In addition, Horii et al. (2006), Pryor and

695 Klemm (2004), and Farmer and Cohen (2008) found deposition velocities for HNO_3 similar to our results. However, emissions for HNO_3 were reported in recent publications (Tarnay et al., 2002; Farmer and Cohen, 2006, 2008). The latter conducted flux measurements of HNO_3 above a pine forest and found a significant contribution of emission fluxes during summer. Those emission could also be induced by the evaporation of NH_4NO_3 from leaf surfaces occurring at higher temperatures (Wyers and Duyzer, 1997; Van Oss et al., 1998), by interactions with hydrochloric acid, or particles deposited or formed on leaf surfaces

700 as discussed by Nemitz et al. (2004).

Deposition velocities for NO and NO_2 were in agreement with values reported in several studies, e.g., mostly ranging between 0.005 and 0.012 cm s^{-1} for NO (Delaria, et al., 2018) and between 0.015 and 0.51 cm s^{-1} for NO_2 (e.g., Rondon et al., 1993; Horii et al., 2004; Chaparro-Suarez et al., 2011; Delaria, et al., 2018, 2020). However, emission fluxes of NO and NO_2 were

705 reported in several publications, e.g., Farmer and Cohen (2006), Horii et al. (2004), and Min et al. (2014) leading to the assumption of the existence of a compensation point (Thoene et al., 1996), but a compensation point for NO and NO_2 is still under discussion (Chaparro-Suarez et al., 2011; Breuninger, et al. 2013; Delaria, et al., 2018, 2020).

Including a soil compensation point in DEPAC, can lead to a reduction in deposition at sites with generally low ΣN_r deposition

710 and at sites with sparse vegetation. For entire campaign, median deposition velocities for tot-NH_4^+ and tot-NO_3^- (3.4 and 4.2 cm s^{-1}, respectively) are likewise comparable to values reported by Wolff et al. (2010). Their values for v_d agreed well with the inverse of R_a. Farmer et al. (2011) and Gordon et al. (2011) reported v_d for NH_4^+ and NO_3^-, respectively. They found an average v_d of 0.48 cm s^{-1} for NO_3^- and 0.19 cm s^{-1} for NH_4^+ around noon.

715 Besides the current implementation of the exchange pathways in DEPAC, deposition estimates could be more accurate if concentration measurements at a higher time resolution and measurements of the LAI would have been available. We did not take measurements of the LAI or other vegetation properties at the measurement site. Still, the interpretation of differences to flux measurements would be challenging since the vegetation inside the flux footprint was not uniform. Inside the footprint, we identified dead wood in southern direction and a mix of rather young and matured trees in easterly direction. Differences

720 in tree age were related to a dieback by bark beetle in the mid-1990s and 2000s (Beudert and Breit, 2014) from which the forest stand is still recovering. Shifting z_0 or d by ±50 %, caused a change of +5.0 %/-3.2 % and +5.6 %/-9.1 %, respectively, in the nitrogen dry deposition after 2.5 years. An incorrect assessment of the modeled LAI by ±50 % had a significant influence on the dry deposition. It led to a change of +18.9 %/-27.2 %. It shows that in further field applications of DEPAC-1D measurements the LAI should be considered, but an incorrect assessment of the LAI would not solely explain the

725 overestimation of DEPAC-1D to TRANC measurements. The main uncertainty of DEPAC-1D fluxes was most likely the usage of monthly integrated DELTA concentrations for the N_r compounds. Thus, instationarities in the timeseries of these compounds happened on timescales of a few seconds were not accounted in deposition modeling. Even with high-resolution

measurements of the QCL, the short-term variability in NH_3 concentrations was not detectable (Wintjen et al., 2022). As stated in Sec. 2.2.3, we did not superimpose monthly concentrations values with synthetic diurnal patterns. Concentrations of N_r
730 compounds are highly variable during the day and depend on various parameters such as turbulence, temperature, relative humidity, precipitation, emission sources, etc. Reproducing influences of those parameters with averaged diurnal cycles about at least weeks or months, is not possible. We found that NH_3 concentration was generally low during winter and assigned with a low variability as found by measurements. During those times, using monthly integrated averages is reasonable (Schrader et al., 2018). However, we probably overestimated modeled fluxes due to the use of monthly averaged concentrations. In order
735 to get at least an impression which N_r compounds' fluxes are probably biased by this approach, we compared monthly averaged fluxes of LOTOS-EUROS (A1) with fluxes calculated by multiplying monthly averaged v_d with their monthly concentration averages (A2) and subsequently corrected them by applying Eq. (9) and (10) of Schrader et al. (2018). Generally, we found that all N_r compounds' fluxes were overestimated by A2 whereas the difference to A1 depends on the investigated N_r compound and season. All N_r compounds had in common that the difference between both approaches was negligible during
740 seasons with small deposition fluxes, for example in winter. Within seasons of large deposition fluxes, significant discrepancies were found, in particular for NH_3. Overall, mean absolute deviations to A1 were 35.0, 0.27, 0.18, 0.92, 2.5, and 2.4 ng N m^{-2} s^{-1} for NH_3, NO_2, NO, HNO_3, NH_4^+, and NO_3^-, respectively.

It should be considered that we used LOTOS-EUROS data for this comparison. Especially for NH_3, NH_4^+, and NO_3^-, their
745 modeled seasonality and concentrations exhibited significant disagreements to DELTA measurements. Thus, the flux overestimations should be seen as highest guess. Measured high resolution concentrations would have led to lower values. Still, the comparison highlights the necessity for high-resolution measurements of N_r compounds. Those measurements should be made for N_r compounds, which probably prevail the exchange dynamics of ΣN_r at a certain site and thereby at least cover time periods with large temporal variations in their concentrations. This procedure was performed for NH_3 and NO_2 at the
750 measurement site.

Devices measuring NH_3, HNO_3, or NO_x with a high sampling rate have high costs, high power consumption, and require regular maintenance, e.g. for NH_3 (Whitehead et al., 2008; Ferrara et al., 2012, 2021; Zöll et al., 2016; Moravek et al., 2019). A setup consisting of such instruments for each N_r compound, installed at various ecosystems is in most cases not affordable.
755 A combination of DELTA and high-resolution sampling devices installed at sites for a limited time period to investigate concentration and flux dynamics may become a proper solution as suggested by Schrader et al. (2018) for NH_3 and could lead to significant improvements in the implemented parameterizations of various N_r compounds. Depending on vegetation and pollution climate, only high-resolution measurements of certain N_r compounds may be of interest. At agricultural sites as an example, only instruments measuring the NH_3 exchange are needed since processes controlling the ΣN_r exchange are most
760 likely driven by a high NH_3 background concentration (Ammann et al., 2012; Brümmer et al., 2013).

4.3 Uncertainties in LOTOS-EUROS

The larger nitrogen deposition values for the measurement site as modeled by LOTOS-EUROS are mostly related the overestimation of NH_3 concentrations. As visualized by Fig. S1, LOTOS-EUROS clearly overestimated observed NH_3
765 concentrations in spring and autumn. Such an overestimation of NH_3 and NH_4^+ in precipitation at forest monitoring sites was identified before for stations in Baden-Württemberg and Bavaria (Schaap et al., 2017). A similar systematic overestimation in southern Germany has also been identified in comparison to novel NH_3 satellite data (Ge et al., 2020). This leads us to believe that the overestimation is for a large part due to shortcomings in the emission information, potentially in combination with the model resolution.

770 The emission inventory used in this study spatially allocates NH_3 manure derived emissions through a procedure in which the animal numbers per region and agricultural land within a region are the two proxies used. Emissions from fertilizer application are allocated solely on land use. Hence, within a region all agricultural land is assumed to emit the same amount of NH_3, although the intensity of the agricultural practice and distribution of housing may vary substantially within such a region. Only south of the station, agricultural lands are located within 7 x 7 km^2 (the model resolution) of the site. This means that in the

775 grid cell of the model, in which the station is located, there is an emission source present contributing an increased NH_3 concentration even when the wind directions are not transporting air from this agricultural region towards the station. The low measured concentrations of N_r compounds show that the site was mostly outside the transport range of nitrogen enriched air masses. A reduction in grid cell size could lead to a more precise localization of potential nitrogen emission sources and a better description of close-range transport and dilution effects. For a simulation covering 2015, we were able to calculate

780 concentrations and fluxes at a higher grid cell resolution (2 x 2 km^2) and compared the results to the standard resolution. In case of the high grid cell resolution, concentrations were lower but only by 2 to 10 % depending on the compound compared to standard resolution. For the whole grid cell, annual N budget of the high-resolution fluxes was higher than the budget of the standard resolution case study, but only by 4.3 % probably due to the relative increase in forest cover. The higher grid cell resolution probably led to improvements in modeling atmospheric turbulence resulting in higher deposition velocities. This

785 example shows that the grid cell resolution of 7 x 7 km^2 is not mainly responsible for the overestimation of the NH_3 concentrations and N_r fluxes.

Nevertheless, the seasonal cycle also indicates that the emissions in spring, which are related to manure and fertilizer application, are too strong. The agricultural fields close to the Bavarian Forest are predominantly extensively managed grass lands. Manure application to grass lands is known to occur much more spread out across the year in comparison to the

790 application for crop production, which mainly occurs before the growing season. Hence, in reality the emission variability maybe prone more to summer conditions favoring fast mixing and dilution of NH_3. Currently, the detailing of crop dependent emissions, the use variable emission fractions within German regions in combination with the recent timing module of Ge et al. (2020) is under investigation to elucidate if these factors are contributing to the observed mismatches.

795 Additional features may also contribute to the observed differences. Whitin LOTOS-EUROS, modeled concentrations were written out for a reference height of 2.5 m above ground, which was lower than the measurement height of the flux tower. Thus, slight differences in micrometeorological data could be expected, for example the difference in relative humidity in the first half of 2016. Differences for that time period were related to the usage of local meteorological data taken at 50 m, with their instrumentation being installed at the 50 m platform. The deviations in u_* as illustrated in Fig. S6 and Fig. 5 were related

800 to differences in measurement heights at which wind speeds and roughness lengths were calculated. The model grid cell consists of various vegetation types each with a unique surface roughness length. We showed that the weighting of the land use classes within the grid cell was not in agreement with the vegetation of the flux foot print affecting micrometeorological variables, e.g. u_*, L, and thereby the calculation of R_a and R_b. Aerosol deposition contributed significantly to overall dry deposition of LOTOS-EUROS as shown in Fig. 7. In particular during winter, v_d of LOTOS-EUROS was greatly enhanced

805 for NO_3^-, NH_4^+, and HNO_3 compared to DEPAC-1D. Above snow-covered surfaces, unstable stratifications prevailed in the simulations. In addition, Figure S6 revealed large discrepancies in u_* to the measurements. Consequently, R_a and R_b were reduced compared to DEPAC-1D resulting in large deposition velocities.

An incorrect setting of the LAI and z_0 can have a significant influence on ΣN_r deposition as shown in the previous chapter. The results of our sensitivity analysis for LAI and z_0 were comparable to values presented recently by van der Graaf et al.

810 (2020), who used satellite-derived LAI and z_0 data from Moderate Resolution Imaging Spectroradiometer (MODIS) to calculate ΣN_r deposition with LOTOS-EUROS for a grid cell size of 7x7 km^2. Overall, they observed changes in ΣN_r dry deposition of up to 30%. However, there was almost no change in ΣN_r dry deposition and in NH_3 concentration observable for

the Bavarian Forest measurement site if LAI and z_0 from MODIS were used. The attempts of van der Graaf et al. (2020) and Ge et al. (2020) did not provide a solution for the general overestimation of the NH$_3$ deposition above southern Germany. It

815   seems that larger scale and temporal discrepancies in modeled NH$_3$ concentrations could be responsible for the disagreement to flux measurements, and overestimation was only partly related to other issues, for example, the grid cell size of 7x7 km^2. Further investigations on these issues are needed.

Summary & Conclusions

We conducted a comparison of total reactive nitrogen (ΣN_r) dry deposition estimates determined by ecological and

820   micrometeorological methods at a remote, mixed forest site for 2.5 years. We determined annual ΣN_r deposition from flux measurements by using the Total Reactive Atmospheric Nitrogen Converter (TRANC) coupled to a chemiluminescence detector (CLD), an in-situ inferential modeling approach using the bidirectional resistance scheme DEPAC (Deposition of Acidifying Compounds) (here called DEPAC-1D), the chemical transport model LOTOS-EUROS (LOng Term Ozone Simulation – EURopean Operational Smog) v2.0, and by applying the canopy budget technique (CBT).

825   We found that modeled ΣN_r concentrations were on average at 5.0 µg N m^{-3}, compared to 3.1 µg N m^{-3} measured with the TRANC for the entire campaign. A comparison to monthly integrated concentrations of compounds contributing to ΣN_r obtained from passive sampler and DELTA (DEnuder of Long-Term Atmospheric sampling) measurements revealed that ammonia (NH$_3$) concentrations were overestimated by the model by a factor of two to three compared to measured values. In addition, NH$_3$ contributed most to the ΣN_r concentration pattern in LOTOS-EUROS whereas NO$_x$ was identified as

830   predominant compound by measurements. Fluxes predicted by LOTOS-EUROS were substantially higher during spring and winter, and the diurnal flux pattern was not in agreement with TRANC fluxes. DEPAC-1D fluxes were close to the measured fluxes in winter, but deposition was clearly overestimated in summer. From May to September, TRANC and DEPAC-1D deposition velocities differed in their response to micrometeorological variables. A further investigation of stomatal vs. non-stomatal deposition pathways needs to be conducted as these are likely factors for discrepancies in modeling vs. measuring.

835   For 2016 and 2017, the following averaged annual ΣN_r dry deposition were found:

- For TRANC measurements, 4.3±0.4 and 4.7±0.2 kg N ha^{-1} a^{-1} were estimated using the Mean-Diurnal-Variation approach in combination with DEPAC-1D and DEPAC-1D only, respectively.
- The application of DEPAC-1D resulted in 5.8±<0.1 kg N ha^{-1} a^{-1}.
- For the site-specific land-use fractions, 6.5±0.3 kg N ha^{-1} a^{-1} was predicted by LOTOS-EUROS

840   - Minimum and maximum dry deposition of the CBT analysis were 3.8±0.5 and 6.7±0.3 kg N ha^{-1} a^{-1}, respectively.

Including wet deposition estimates from nearby wet-only samplers in the budget calculation, resulted in annual total nitrogen depositions between 11.5 and 14.6 kg N ha^{-1} a^{-1} and between 11.7 and 14.8 kg N ha^{-1} a^{-1} for 2016 and 2017, respectively, thereby being close to the upper limit of the critical load ranges for deciduous and coniferous forests implying that the forest is just at the limit of receiving too much nitrogen from the atmosphere.

845   Differences between DEPAC-1D and TRANC measurements could be related to erroneous parametrizations in the exchange pathways of reactive gases, the usage of low-resolution input data, or the missing exchange pathway with soil. Besides possible uncertainty sources in DEPAC-1D, dry deposition estimates of both gap-filling approaches were similar showing that DEPAC-1D (and by extension, inferential modeling in general) is a valuable gap-filling tool at sites with prevailing N deposition. The difference to LOTOS-EUROS was mainly related to an overestimation of NH$_3$ concentrations. A larger-scale aspect may be

850   responsible for that issue since the general overestimation of NH$_3$ concentrations has still not been solved by several attempts. We found that all estimates were in similar within reasonable margins. However, further comparisons of flux measurements and model applications are needed to investigate exchange characteristics of ΣN_r and its individual compounds, if possible, simultaneously and at different ecosystems. Measuring several N$_r$ compounds and ΣN_r at a high time resolution is probably

855   not affordable due to maintenance costs, high technical requirements, and time-consuming processing of the acquired data. A solution could be continuous monitoring of N_r compounds by low-cost samplers complemented by high-frequency measurements of ΣN_r and selected compounds like NH_3 for a limited time, which will result in a better understanding of exchange processes and thus in an improvement of deposition models (cf. Schrader et al., 2018).

860

Code and data availability. All data are available upon request from the first author of this study (pascal.wintjen@thuenen.de). Concentration, flux, and micrometeorological data from measurements and ecological information about the site are included in the following repository: https://zenodo.org/record/5841074 (Brümmer et al., 2022a). Also, Python 3.7 code for flux data analysis can be requested from the first author.

865

Author contributions. PW, FS, MS, and CB conceived the study. PW wrote the manuscript, carried out the measurements at the forest site, and the comparison of measured and modeled flux data and interpretation. FS evaluated meteorological measurements and set up DEPAC-1D. MS and RK provided insights in interpreting LOTOS-EUROS results. BB conducted canopy throughfall and wet deposition measurements. CB installed the instruments at the site. The results were thoroughly discussed with all authors, and FS, MS, BB, RK, and CB contributed to the manuscript.

875

Competing interests. The authors declare that they have no conflict of interest.

880   *Acknowledgements.* We thank Undine Zöll for scientific and logistical help to the measurements, Jeremy Rüffer and Jean-Pierre Delorme for excellent technical support, Ute Tambor, Andrea Niemeyer, and Dr. Daniel Ziehe for conducting laboratory analyses of denuder and filter samples, and the Bavarian Forest Nationalpark (NPBW) Administration, namely Wilhelm Breit and Ludwig Höcker for technical and logistical support at the measurement site.

885

Financial support. This work has been funded by the German Environment Agency (UBA) (project FORESTFLUX, support code FKZ 3715512110) and by the German Federal Ministry of Education and Research (BMBF) within the framework of the Junior Research Group NITROSPHERE (support code FKZ 01LN1308A).

References

890   Ahrends, B., Schmitz, A., Prescher, A.-K., Wehberg, J., Geupel, M., Henning, A., and Meesenburg, H.; Comparison of Methods for the Estimation of Total Inorganic Nitrogen Deposition to Forests in Germany, Frontiers in Forests and Global Change, 3, 1-22, doi:10.3389/ffgc.2020.00103, 2020.

Ammann, C., Wolff, V., Marx, O., Brümmer, C., and Neftel, A.: Measuring the biosphere-atmosphere exchange of total
895   reactive nitrogen by eddy covariance, Biogeosciences, 9, 4247–4261, doi:10.5194/bg-9-4247-2012, 2012.

Beudert, B. and Breit, W.: Integrated Monitoring Programm an der Meßstelle Forellenbach im Nationalpark Bayerischer Wald,
Untersuchungen zum Stickstoffeintrag und zum wassergebundenen Stickstoffhaushalt des Forellenbachgebiets,
Förderkennzeichen 351 01 012. Nationalparkverwaltung Bayerischer Wald, Sachgebiet IV, techreport, Umweltbundesamt,
Dessau-Roßlau,   Germany,   available   at:
900   http://www.umweltbundesamt.de/sites/default/files/medien/370/dokumente/ece_im_forellenbach_berichtsjahr_2009.pdf (last
access: 14 March 2022), 2010.

Beudert, B. and Breit, W.: Kronenraumbilanzen zur Abschätzung der Stickstoffgesamtdeposition in Waldökosysteme des
Nationalparks   Bayerischer   Wald,   techreport,   Umweltbundesamt,   Dessau-Roßlau,   Germany,   available   at:
https://www.umweltbundesamt.de/sites/default/files/medien/370/dokumente/kronenraumbilanzen_stickstoffgesamtdepositio
905   n_nationalpark_bayerisches_wald_-_berichtsjahr_2013_im_forellenbach.pdf (last access: 14 March 2022), 2014.

Beudert, B., and Gietl, G.: Long-term monitoring in the Große Ohe catchment, Bavarian Forest National Park, Silva
Gabreta, 21, 5-27, https://www.npsumava.cz/wp-content/uploads/2019/06/sg_21_1_beudertgietl.pdf (last access: 14 March
2022), 2015.

Bobbink, R., Hornung, M. and Roelofs, J. G. M.: The effects of air-borne nitrogen pollutants on species diversity in natural
910   and semi-natural European vegetation, Journal of Ecology, 86, 717–738, doi:10.1046/j.1365-2745.1998.8650717.x, 1998.

Bobbink, R. and Hettelingh, J.-P.: Review and revision of empirical critical loads and dose-response relationships. National
Institute   for   Public   Health   and   the   Environment   (RIVM),   RIVM   Report,
https://www.rivm.nl/bibliotheek/rapporten/680359002.pdf (last access: 14 March 2022), 2011.

Breuninger, C., Meixner, F. X., and Kesselmeier, J.: Field investigations of nitrogen dioxide (NO_2) exchange between plants
915   and the atmosphere, Atmospheric Chemistry and Physics, 13, 773–790, doi:10.5194/acp-13-773-2013, 2013.

Brümmer, C., Marx, O., Kutsch, W., Ammann, C., Wolff, V., Flechard, C. R., and Freibauer, A.: Fluxes of total reactive
atmospheric nitrogen (ΣN_r) using eddy covariance above arable land, Tellus B: Chemical and Physical Meteorology, 65,
19770, doi:10.3402/tellusb.v65i0.19770, 2013.

Brümmer, C., Rüffer, J. J., Delorme, J.-P., Wintjen, P., Schrader, F., Beudert, B., Schaap, M., and Ammann, C.: Reactive
920   nitrogen fluxes over peatland and forest ecosystems using micrometeorological measurement techniques, Earth System
Science Data, 14, 743-761, doi:10.5194/essd-14-743-2022, 2022.

Brümmer, C., Rüffer, J. J., Delorme, J.-P., Wintjen, P., Schrader, F., Beudert, B., Schaap, M., and Ammann, C.: Reactive
nitrogen fluxes over peatland (Bourtanger Moor) and forest (Bavarian Forest National Park) using micrometeorological
measurement techniques (1.1) [Data set]. Zenodo. doi:10.5281/zenodo.5841074, 2022a.

925   Butterbach-Bahl, K., Gasche, R., Breuer, L., and Papen, H.: Fluxes of NO and N_2O from temperate forest soils: impact of
forest type, N deposition and of liming on the NO and N_2O emissions, Nutrient Cycling in Agroecosystems, 48, 79–90,
doi:10.1023/a:1009785521107, 1997.

Chaparro-Suarez, I., Meixner, F., and Kesselmeier, J.: Nitrogen dioxide (NO_2) uptake by vegetation controlled by atmospheric
concentrations and plant stomatal aperture, Atmospheric Environment, 45, 5742–5750, doi:10.1016/j.atmosenv.2011.07.021,
930   2011

Damgaard, C., Jensen, L., Frohn, L. M., Borchsenius, F., Nielsen, K. E., Ejrnæs, R. and Stevens, C. J.: The effect of nitrogen
deposition on the species richness of acid grasslands in Denmark: A comparison with a study performed on a European scale,
Environmental Pollution, 159, 1778-1782, doi:10.1016/j.envpol.2011.04.003, 2011.

Delaria, E. R., Vieira, M., Cremieux, J., and Cohen, R. C.: Measurements of NO and NO_2 exchange between the atmosphere
935   and Quercus agrifolia, Atmospheric Chemistry and Physics, 18, 14 161–14 173, doi:10.5194/acp-18-14161-2018, 2018.

Delaria, E. R., Place, B. K., Liu, A. X., and Cohen, R. C.: Laboratory measurements of stomatal NO_2 deposition to native California trees and the role of forests in the NO_x cycle, Atmospheric Chemistry and Physics, 20, 14 023–14 041, doi:10.5194/acp-20-14023-2020, 2020.

de Vries, W., Reinds, G. J., and Vel, E.: Intensive monitoring of forest ecosystems in Europe: 2: Atmospheric deposition and
940   its impacts on soil solution chemistry, Forest Ecology and Management, 174, 97–115, doi:10.1016/S0378-1127(02)00030-0, 2003.

Dirnböck, T., Grandin, U., Bernhardt-Römermann, M., Beudert, B., Canullo, R., Forsius, M., Grabner, M.-T., Holmberg, M., Kleemola, S., Lundin, L., Mirtl, M. Neumann, M., Pompei, E., Salemaa, M., Starlinger, F., Staszewski, T., and Uziębło, A. K.: Forest floor vegetation response to nitrogen deposition in Europe, Global Change Biology, 20, 429-440, doi:
945   10.1111/gcb.12440 , 2014.

Dirnböck, T., Pröll, G., Austnes, K., Beloica, J., Beudert, B., Canullo, R., De Marco, A., Fornasier, M. F., Futter, M., Goergen, K., Grandin, U., Holmberg, M., Lindroos, A.-J., Mirtl, M., Neirynck, J., Pecka, T., Nieminen, T. M., Nordbakken, J.-F., Posch, M., Reinds, G.-J., Rowe, E. C., Salemaa, M., Scheuschner, T., Starlinger, F., Uziębło, A. K., Valinia, S., Weldon, J., Wamelink, W. G. W., and Forsius, M.: Currently legislated decreases in nitrogen deposition will yield only limited plant species recovery
950   in European forests, Environmental research letters, 13, 125010, doi: 10.1088/1748-9326/aaf26b, 2018.

Draaijers, G. P. J. and Erisman, J. W.: A canopy budget model to assess atmospheric deposition from throughfall measurements, Water, Air, Soil Pollution, 85, 2253–2258, doi: 10.1007/BF01186169, 1995.

Emberson, L.D., Ashmore, M. R., Simpson, D., Tuovinen, J.-P. and Cambridge, H. M.: Towards a model of ozone deposition and stomatal uptake over Europe, EMEP/MSC-W 6/2000, Norwegian Meteorological Institute, Oslo, 2000a.

955   Emberson, L. D., Ashmore, M. R., Cambridge, H. M., Simpson, D., and Tuovinen, J. P.: Modelling stomatal ozone flux across Europe, Environmental Pollution, 109, 403–13, doi:10.1016/S0269-7491(00)00043-9, 2000b.

Erisman, J. W., Van Pul, A., and Wyers, P.: Parametrization of surface resistance for the quantification of atmospheric deposition of acidifying pollutants and ozone, Atmospheric Environment, 28, 2595–2607, doi:10.1016/1352-2310(94)90433-2, 1994.

960   Erisman, J. W., Galloway, J., Seitzinger, S., Bleeker, A. and Butterbach-Bahl, K.: Reactive nitrogen in the environment and its effect on climate change, Current Opinion in Environmental Sustainability, 3, 281-290, doi: 10.1016/j.cosust.2011.08.012., 2011.

Erisman, J. W., Galloway, J. N., Seitzinger, S., Bleeker, A., Dise, N. B., Petrescu, A. M., Leach, A. M. and de Vries, W.: Consequences of human modification of the global nitrogen cycle, Philosophical Transactions of the Royal Society London
965   B: Biological Sciences, 368, 201301116, doi: 10.1098/rstb.2013.0116, 2013.

Falge, E., Baldocchi, D., Olson, R., Anthoni, P., Aubinet, M., Bernhofer, C., Burba, G., Ceulemans, R., Clement, R., Dolman, H., Granier, A., Gross, P., Grünwald, T., Hollinger, D., Jensen, N.-O., Katul, G., Keronen, P., Kowalski, A., Lai, C. T., Law, B. E., Meyers, T., Moncrieff, J., Moors, E., Munger, J., Pilegaard, K., Üllar Rannik, Rebmann, C., Suyker, A., Tenhunen, J., Tu, K., Verma, S., Vesala, T., Wilson, K., and Wofsy, S.: Gap filling strategies for defensible annual sums of net ecosystem
970   exchange, Agricultural and Forest Meteorology, 107, 43–69, doi:10.1016/S0168-1923(00)00225-2, 2001.

Farmer, D. K., Wooldridge, P. J., and Cohen, R. C.: Application of thermal-dissociation laser induced fluorescence (TD-LIF) to measurement of HNO_3, Σalkyl nitrates, Σperoxy nitrates, and NO_2 fluxes using eddy covariance, Atmospheric Chemistry and Physics, 6, 3471–3486, doi:10.5194/acp-6-3471-2006, 2006.

Farmer, D. K. and Cohen, R. C.: Observations of HNO_3, ΣAN, ΣPN and NO_2 fluxes: evidence for rapid HO_x chemistry within
975   a pine forest canopy, Atmospheric Chemistry and Physics, 8, 3899–3917, doi:10.5194/acp-8-3899-2008, 2008.

Farmer, D. K., Kimmel, J. R., Phillips, G., Docherty, K. S., Worsnop, D. R., Sueper, D., Nemitz, E., and Jimenez, J. L.: Eddy covariance measurements with high-resolution time-of-flight aerosol mass spectrometry: a new approach to chemically resolved aerosol fluxes, Atmos. Meas. Tech., 4, 1275–1289, doi:10.5194/amt-4-1275-2011, 2011.

Farmer, D. K., Chen, Q., Kimmel, J. R., Docherty, K. S., Nemitz, E., Artaxo, P. A., Cappa, C. D., Martin, S. T., and Jiminez,
980   J. L.: Chemically Resolved Particle Fluxes Over Tropical and Temperate Forests, Aerosol Science and Technology, 47:7, 818-
830, doi:10.1080/02786826.2013.791022, 2013.

Ferm, M.: A Sensitive Diffusional Sampler, Report L91-172, Swedish Environmental Research Institute, Gothenburg, 1991.

Ferrara, R. M., Loubet, B., Di Tommassi, P., Bertolini, T., Magliulo, V., Cellier, P., Eugster, W., and Rana, G.: Eddy
covarinance measurement of ammonia fluxes: Comparison of high frequency correction methodologies, Agricultural and
985   Forest Meteorology, 158-159, 30-42, doi:10.1016/j.agrformet.2012.02.001, 2012.

Ferrara, R. M., Di Tommassi, P., Farmulari, D., and Rana G.: Limitations of an Eddy-Covariance System in Measuring Low
Ammonia Fluxes, Boundary-Layer Meteorology, 180, 173-186, doi:10.1007/s10546-021-00612-6, 2021.

Flechard, C. R., Nemitz, E., Smith, R. I., Fowler, D., Vermeulen, A. T., Bleeker, A., Erisman, J. W., Simpson, D., Zhang, L.,
Tang, Y. S., and Sutton, M. A.: Dry deposition of reactive nitrogen to European ecosystems: a comparison of inferential models
990   across the NitroEurope network, Atmos. Chem. Phys., 11, 2703–2728, doi:10.5194/acp-11-2703-2011, 2011.

Flechard, C. R., Ibrom, A., Skiba, U. M., de Vries, W., van Oijen, M., Cameron, D. R., Dise, N. B., Korhonen, J. F. J.,
Buchmann, N., Legout, A., Simpson, D., Sanz, M. J., Aubinet, M., Loustau, D., Montagnani, L., Neirynck, J., Janssens, I. A.,
Pihlatie, M., Kiese, R., Siemens, J., Francez, A.-J., Augustin, J., Varlagin, A., Olejnik, J., Juszczak, R., Aurela, M., Berveiller,
D., Chojnicki, B. H., Dammgen, U., Delpierre, N., Djuricic, V., Drewer, J., Dufrene, E., Eugster, W., Fauvel, Y., Fowler, D.,
995   Frumau, A., Granier, A., Gross, P., Hamon, Y., Helfter, C., Hensen, A., Horvath, L., Kitzler, B., Kruijt, B., Kutsch, W. L.,
Lobo-do Vale, R., Lohila, A., Longdoz, B., Marek, M. V., Matteucci, G., Mitosinkova, M., Moreaux, V., Neftel, A., Ourcival,
J.-M., Pilegaard, K., Pita, G., Sanz, F., Schjoerring, J. K., Sebastia, M.-T., Tang, Y. S., Uggerud, H., Urbaniak, M., van Dijk,
N., Vesala, T., Vidic, S., Vincke, C., Weidinger, T., Zechmeister-Boltenstern, S., Butterbach-Bahl, K., Nemitz, E., and Sutton,
M. A.: Carbon–nitrogen interactions in European forests and semi-natural vegetation – Part 1: Fluxes and budgets of carbon,
1000   nitrogen and greenhouse gases from ecosystem monitoring and modelling, Biogeosciences, 17, 1583–1620, doi:10.5194/bg-
17-1583-2020, 2020.

Fowler, D., Coyle, M., Skiba, U., Sutton, M. A., Cape, J. N., Reis, S., Sheppard, L. J., Jenkins, A., Grizzetti, B., Galloway, J.
N., Vitousek, P., Leach, A., Bouwman, A. F., Butterbach-Bahl, K., Dentener, F., Stevenson, D., Amann, M. and Voss, M.:
The global nitrogen cycle in the twenty-first century, Philosophical Transactions of the Royal Society B: Biological Sciences,
1005   368, 20130164, doi: 10.1098/rstb.2013.0164, 2013.

Galloway, J. N., Aber, J. D., Erisman, J. W., Seitzinger, S. P., Howarth, R. W., Cowling, E. B. and Cosby, B. J.: The Nitrogen
Cascade, BioScience, 53, 341-356, doi: 10.1641/0006-3568(2003)053[0341:TNC]2.0.CO;2, 2003.

Garland, J. A.: The Dry Deposition of Sulphur Dioxide to Land and Water Surfaces, Proceedings of the Royal Society A:
Mathematical, Physical and Engineering Sciences, 354, 245–268, doi:10.1098/rspa.1977.0066, 1977.

1010   Ge, X., Schaap, M., Kranenburg, R., Segers, A., Reinds, G. J., Kros, H., and de Vries, W.: Modeling atmospheric ammonia
using agricultural emissions with improved spatial variability and temporal dynamics, Atmos. Chem. Phys., 20, 16055–16087,
doi:10.5194/acp-20-16055-2020, 2020.

Geddes, J. A. and Murphy, J. G.: Observations of reactive nitrogen oxide fluxes by eddy covariance above two midlatitude
North American mixed hardwood forests, Atmospheric Chemistry and Physics, 14, 2939–2957, doi:10.5194/acp-14-2939-
1015   2014, 2014.

Gordon, M., Staebler, R. M., Liggio, J., Vlasenko, A., Li, S.-M., and Hayden, K.: Aerosol flux measurements above a mixed
forest at Borden, Ontario, Atmos. Chem. Phys., 11, 6773–6786, doi:10.5194/acp-11-6773-2011, 2011.

Hansen, K., Sørensen, L. L., Hertel, O., Geels, C., Skjøth, C. A., Jensen, B., and Boegh, E.: Ammonia emissions from
deciduous forest after leaf fall, Biogeosciences, 10, 4577–4589, doi:10.5194/bg-10-4577-2013, 2013.

1020   Hansen, K., Pryor, S. C., Boegh, E., Hornsby, K. E., Jensen, B., and Sørensen, L. L.: Background concentrations and fluxes
         of atmospheric ammonia over a deciduous forest, Agricultural and Forest Meteorology, 214-215, 380–392, doi:
         10.1016/j.agrformet.2015.09.004, 2015.

         Hettelingh, J.-P., Posch, M., De Smet, P. A. M. and Downing, R. J.: The use of critical loads in emission reduction agreements
         in Europe, Water, Air, and Soil Pollution., 85, 2381-2385, doi:10.1007/BF01186190, 1995.

1025   Hettelingh, J.-P., Posch, M., Velders, G. J. M., Ruyssenaars, P., Adams, M., de Leeuw, F., Lükewille, A., Maas, R., Sliggers,
         J. and Slootweg, J.: Assessing interim objectives for acidification, eutrophication and ground-level ozone of the EU National
         Emission Ceilings Directive with 2001 and 2012 knowledge, Atmospheric Environment, 75, 129-140,
         doi:10.1016/j.atmosenv.2013.03.060, 2013.

         Horii, C. V., Munger, J. W., Wofsy, S. C., Zahniser, M., Nelson, D., and McManus, J. B.: Fluxes of nitrogen oxides over a
1030   temperate deciduousforest, Journal of Geophysical Research: Atmospheres, 109, doi:10.1029/2003JD004326, 2004.

         Horii, C. V., Munger, J. W., Wofsy, S. C., Zahniser, M., Nelson, D., and McManus, J. B.: Atmospheric reactive nitrogen
         concentration and flux budgets at a Northeastern US forest site, Agricultural and Forest Meteorology, 136, 159–174,
         doi:10.1016/j.agrformet.2006.03.005, 2006.

         Jarvis, P. G.: The Interpretation of the Variations in Leaf Water Potential and Stomatal Conductance Found in Canopies in the
1035   Field, Philos. T. R. Soc. B, 273, 593–610, doi:10.1098/rstb.1976.0035, 1976.

         Jensen, N. and Hummelshøj, P.: Derivation of canopy resistance for water vapor fluxes over a spruce forest, using a new
         technique for the viscous sublayer resistance (correction to vol. 73, p. 339, 1995), Agricultural and Forest Meteorology, 85,
         289, doi:10.1016/S0168-1923(97)00024-5, 1997.

         Jensen, N. O. and Hummelshøj, P.: Derivation of canopy resistance for water-vapor fluxes over a spruce forest, using a new
1040   technique for the viscous sublayer resistance, Agricultural and Forest Meteorology, 73, 339–352, doi:10.1016/0168-
         1923(94)05083-I, 1995.

         Krupa, S. V.: Effects of atmospheric ammonia (NH$_3$) on terrestrial vegetation: a review, Environmental Pollution, 124, 179-
         211, doi: 10.1016/S0269-7491(02)00434-7, 2003.

         Kuenen, J., Dellaert, S., Visschedijk, A., Jalkanen, J.-P., Super, I., and Denier van der Gon, H.: CAMS-REG-v4: a state-of-
1045   the-art high-resolution European emission inventory for air quality modelling, Earth Syst. Sci. Data Discuss. [preprint],
         doi:10.5194/essd-2021-242, in review, 2021

         Li, Y., Schichtel, B. A., Walker, J. T., Schwede, D. B., Chen, X., Lehman, C. M. B., Puchalski, M. A., Gay, D. A., and Collett,
         J. L.; Increasing importance of deposition of reduced nitrogen in the United States, Proceedings of the National Academy of
         Sciences, 113, 5874-5879, doi: 10.1073/pnas.1525736113, 2016.

1050   LTER: Long Term Ecological Research (LTER) network, available at: https://deims.org/993ed2fc-1cb0-4810-a619-
         8bcf78b6ecee (last access: 14 March 2022), 2022.

         Marx, O., Brümmer, C., Ammann, C., Wolff, V., and Freibauer, A.: TRANC – a novel fast-response converter to measure
         total reactive atmospheric nitrogen, Atmospheric Measurement Techniques, 5, 1045–1057, doi:10.5194/amt-5-1045-2012,
         2012.

1055   Manders-Groot, A. M. M., Segers, A. J., and Jonkers, S.: LOTOS-EUROS v2.0 Reference Guide, TNO report TNO2016
         R10898, TNO, Utrecht, The Netherlands, https://lotos-euros.tno.nl/media/10360/reference_guide_v2-0_r10898.pdf (last
         access: 14 March 2022), 2016.

         Manders, A. M. M., Builtjes, P. J. H., Curier, L., Denier van der Gon, H. A. C., Hendriks, C., Jonkers, S., Kranenburg, R.,
         Kuenen, J. J. P.,Segers, A. J., Timmermans, R. M. A., Visschedijk, A. J. H., Wichink Kruit, R. J., van Pul, W. A. J., Sauter, F.
1060   J., van der Swaluw, E., Swart, D. P. J., Douros, J., Eskes, H., van Meijgaard, E., van Ulft, B., van Velthoven, P., Banzhaf, S.,
         Mues, A. C., Stern, R., Fu, G., Lu,S., Heemink, A., van Velzen, N., and Schaap, M.: Curriculum vitae of the LOTOS–EUROS
         (v2.0) chemistry transport model, Geoscientific Model Development, 10, 4145–4173, doi:10.5194/gmd-10-4145-2017, 2017.

Milford, C., Hargreaves, K. J., Sutton, M. A., Loubet, B., and Cellier, P.: Fluxes of NH_3 and CO_2 over upland moorland in the vicinity of agricultural land, Journal of Geophysical Research: Atmospheres, 106, 24 169–24 181, doi:10.1029/2001jd900082, 2001.

1065

Min, K.-E., Pusede, S. E., Browne, E. C., LaFranchi, B. W., Wooldridge, P. J., and Cohen, R. C.: Eddy covariance fluxes and vertical concentration gradient measurements of NO and NO_2 over a ponderosa pine ecosystem: observational evidence for within canopy chemical removal of NO_x, Atmospheric Chemistry and Physics, 14, 5495–5512, doi:10.5194/acp-14-5495-2014, 2014.

1070 Moravek, A., Singh, S., Pattey, E., Pelletier, L., and Murphy, J. G.: Measurements and quality control of ammonia eddy covariance fluxes: A new strategy for high frequency attenuation correction, Atmospheric Measurement Techniques, 12, 6059–6078, doi:10.5194/amt-12-6059-2019, 2019.

Munger, J. W., Wofsy, S. C., Bakwin, P. S., Fan, S. M., Goulden, M. L., Daube, B. C., Goldstein, A. H., Moore, K. E., and Fitzjarrald, D. R.: Atmospheric deposition of reactive nitrogen oxides and ozone in a temperate deciduous forest and a subarctic

1075 woodland: 1. Measurements and mechanisms, Journal of Geophysical Research-Atmospheres, 101, 12 639–12 657, doi:10.1029/96JD00230, 1996.

Nemitz, E., Sutton, M. A., Wyers, G. P., and Jongejan, P. A. C.: Gas-particle interactions above a Dutch heathland: I. Surface exchange fluxes of NH_3, SO_2, HNO_3 and HCl, Atmospheric Chemistry and Physics, 4, 989–1005, doi:10.5194/acp-4-989-2004, 2004.

1080 Paulissen, M.P.C.P., Bobbink, R., Robat, S.A., and Verhoeven, J. T. A.: Effects of Reduced and Oxidised Nitrogen on Rich-Fen Mosses: a 4-Year Field Experiment., Water, Air, & Soil Pollution, 227, 18, doi:10.1007/s11270-015-2713-y, 2016.

Paulson, C. A.: The Mathematical Representation of Wind Speed and Temperature Profiles in the Unstable Atmospheric Surface Layer, Journal of Applied Meteorology, 9, 857–861, doi:10.1175/1520-0450(1970)009<0857:Tmrows>2.0.Co;2, 1970.

1085 Pryor, S. C., Barthelmie, R. J., Sørensen, L. L., and Jensen, B.: Ammonia concentrations and fluxes over a forest in the midwestern USA, Atmospheric Environment, 35, 5645-5656, doi:10.1016/S1352-2310(01)00259-X, 2001.

Pryor, S. and Klemm, O.: Experimentally derived estimates of nitric acid dry deposition velocity and viscous sub-layer resistance at a conifer forest, Atmospheric Environment, 38, 2769–2777, doi:10.1016/j.atmosenv.2004.02.038, 2004.

Reichstein, M., Falge, E., Baldocchi, D., Papale, D., Aubinet, M., Berbigier, P., Bernhofer, C., Buchmann, N., Gilmanov, T.,

1090 Granier, A., Grünwald, T., Havránková, K., Ilvesniemi, H., Janous, D., Knohl, A., Laurila, T., Lohila, A., Loustau, D., Matteucci, G., Meyers, T., Miglietta, F., Ourcival, J.-M., Pumpanen, J., Rambal, S., Rotenberg, E., Sanz, M., Tenhunen, J., Seufert, G., Vaccari, F., Vesala, T., Yakir, D., and Valentini, R.: On the separation of net ecosystem exchange into assimilation and ecosystem respiration: review and improved algorithm, Global Change Biology, 11, 1424–1439, doi:10.1111/j.1365-2486.2005.001002.x, 2005.

1095 Rondon, A., Johansson, C., and Granat, L.: Dry Deposition of Nitrogen-Dioxide and Ozone to Coniferous Forests, Journal of Geophysical Research-Atmospheres, 98, 5159–5172, doi:10.1029/92jd02335, 1993.

Rosenkranz, P., Brüggemann, N., Papen, H., Xu, Z., Seufert, G., and Butterbach-Bahl, K.: N2O, NO and CH4 exchange, and microbial N turnover over a Mediterranean pine forest soil, Biogeosciences, 3, 121–133, doi:10.5194/bg-3-121-2006, 2006.

Roth, M., Müller-Meißner, A., Michiels, H.-G., and Hauck, M.: Vegetation changes in the understory of nitrogen-sensitive

1100 temperate forests over the past 70 years, Forest Ecology and Management, 503, 119754, doi:10.1016/j.foreco.2021.119754 2022.

Rummel, U., Ammann, C., Gut, A., Meixner, F. X., and Andreae, M. O.: Eddy covariance measurements of nitric oxide flux within an Amazonian rain forest, Journal of Geophysical Research-Atmospheres, 107, LBA 17–1–LBA 17–9, doi:10.1029/2001JD000520, 2002.

1105   Sauter, F., Sterk, M., van der Swaluw, E., Wichink Kruit, R., de Vries, W., and van Pul, A.: The OPS-model: Description of OPS 5.0.0.0, RIVM, Bilthoven, https://www.rivm.nl/media/ops/OPS-model.pdf (last access: 14 March 2022), 2020.

Saylor, R. D., Baker, B. D., Lee, P., Tong, D., Pan, L., and Hicks, B. B.: The particle dry deposition component of total deposition from air quality models: right, wrong or uncertain?, Tellus B: Chemical and Physical Meteorology, 71, 1550324, doi: 10.1080/16000889.2018.1550324, 2019.

1110   Schaap, M., Wichink Kruit, R., Hendriks, C., Kranenburg, R., Segers, A., Builtjes, P., and Banzhaf, S.: Modelling and assessment of acidifying and eutrophying atmospheric deposition to terrestrial ecosystems (PINETI-2): Part I: Atmospheric deposition to German natural and semi-natural ecosystems during 2009, 2010 and 2011, techinal report, Umweltbundesamt, Dessau-Roßlau, Germany, https://www.umweltbundesamt.de/sites/default/files/medien/1410/publikationen/2017-08-15_texte_62-2017_pineti2-teil1.pdf (last access: 14 March 2022), 2017.

1115   Schaap. M., Hendriks, C., Kranenburg, R., Kuenen, J., Segers, A., Schlutow, A., Nagel, H.-D., Ritter, A., and Banzhaf, S.: PINETI-3: Modellierung atmosphärischer Stoffeinträge von 2000 bis 2015 zur Bewertung der ökosystem-spezifischen Gefährdung von Biodiversität durch Luftschadstoffe in Deutschland, technical report, Umweltbundesamt, Dessau-Roßlau, Germany, https://www.umweltbundesamt.de/sites/default/files/medien/1410/publikationen/2018-10-17_texte_79-2018_pineti3.pdf (last access: 14 March 2022), 2018.

1120   Schrader, F. and Brümmer, C.: Land Use Specific Ammonia Deposition Velocities: a Review of Recent Studies (2004–2013), Water, Air, and Soil Pollution, 225, 2114, doi:10.1007/s11270-014-2114-7, 2014.

Schrader, F., Brümmer, C., Flechard, C. R., Wichink Kruit, R. J., van Zanten, M. C., Zöll, U., Hensen, A., and Erisman, J. W.: Non-stomatal exchange in ammonia dry deposition models: comparison of two state-of-the-art approaches, Atmospheric Chemistry and Physics, 16, 13417–13430, doi:10.5194/acp-16-13417-2016, 2016.

1125   Schrader, F., Schaap, M., Zöll, U., Kranenburg, R., and Brümmer, C.: The hidden cost of using low-resolution concentration data in the estimation of NH_3 dry deposition fluxes, Scientific Reports, 8, 969, doi:10.1038/s41598-017-18021-6, 2018.

Schwede, D., Zhang, L., Vet, R., and Lear, G.: An intercomparison of the deposition models used in the CASTNET and CAPMoN networks, Atmospheric Environment, 45, 1337–1346, doi: 10.1016/j.atmosenv.2010.11.050, 2011.

Sparks, J. P., Monson, R. K., Sparks, K. L., and Lerdau, M.: Leaf uptake of nitrogen dioxide (NO_2) in a tropical wet forest:
1130   implications for tropospheric chemistry, Oecologia, 127, 214–221, doi:10.1007/s004420000594, 2001.

Staelens, J., Houle, D.and De Schrijver, A., Neirynck, J., and Verheyen, K.: Calculating Dry Deposition and Canopy Exchange with the Canopy Budget Model: Review of Assumptions and Application to Two Deciduous Forests,Water, Air, and Soil Pollution, 191, 149–169, doi:10.1007/s11270-008-9614-2, 2008.

Sutton, M. A. and Fowler, D.: A Model for Inferring Bi-directional Fluxes of Ammonia Over Plant Canopies, in: Proceedings
1135   of the WMO conference on the measurement and modelling of atmospheric composition changes including pollutant transport, pp. 179–182, WMO/GAW(Gobal Atmosphere Watch)-91, Geneva, Switzerland, 1993.

Sutton, M. A., Tang, Y. S., Miners, B., and Fowler, D.: A New Diffusion Denuder System for Long-Term, Regional Monitoring of Atmospheric Ammonia and Ammonium, Water, Air and Soil Pollution: Focus, 1, 145–156, doi:10.1023/a:1013138601753, 2001.

1140   Sutton, M. A., Howard, C. M., Erisman, J. W., Billen, G., Bleeker, A., Grennfelt, P., van Grinsven, H. and Grizzetti, B.: The European Nitrogen Assessment: sources, effects and policy perspectives, Cambridge University Press, Cambridge, UK, 2011.

Sutton, M. A., Reis, S., Riddick, S. N., Dragosits, U., Nemitz, E., Theobald, M. R., Tang, Y. S., Braban, C. F. , Vieno, M., Dore, A. J., Mitchell, R. F., Wanless, S., Daunt, F., Fowler, D., Blackall, T. D., Milford, C., Flechard, C. R., Loubet, B., Massad, R., Cellier, P., Personne, E., Coheur, P. F., Clarisse, L. Van Damme, M., Ngadi, Y., Clerbaux, C., Skjoth, C. A.,
1145   Geels, C., Hertel, O., Wichink Kruit, R. J., Pinder, R. W., Bash, J. O., Walker, J. T., Simpson, D., Horvath, L., Misselbrook, T. H., Bleeker, A., Dentener, F. and de Vries, W.: Towards a climate-dependent paradigm of ammonia emission and deposition,

Philosophical Transactions of the Royal Society of London. Series B.: Biological Sciences, 368, 20130166, doi: 10.1098/rstb.2013.0166, 2013.

Tang, Y. S., Simmons, I., van Dijk, N., Di Marco, C., Nemitz, E., Dämmgen, U., Gilke, K., Djuricic, V., Vidic, S., Gliha, Z.,
1150 Borovecki, D., Mitosinkova, M., Hanssen, J. E., Uggerud, T. H., Sanz,M. J., Sanz, P., Chorda, J. V., Flechard, C. R., Fauvel, Y., Ferm, M., Perrino, C., and Sutton, M. A.: European scale application of atmospheric reactive nitrogen measurements in a low-cost approach to infer dry deposition fluxes, Agriculture, Ecosystems and Environment, 133, 183–195, doi:10.1016/j.agee.2009.04.027, 2009.

Tarnay, L. W., Gertler, A., and Taylor, G. E.: The use of inferential models for estimating nitric acid vapor deposition to semi-
1155 arid conifer-ous forests, Atmospheric Environment, 36, 3277–3287, doi:10.1016/S1352-2310(02)00303-5, 2002.

Thoene, B., Rennenberg, H., and Weber, P.: Absorption of atmospheric NO_2 by spruce (Picea abies) trees, New Phytologist, 134, 257–266, doi:10.1111/j.1469-8137.1996.tb04630.x, 1996.

Trebs, I., Metzger, S., Meixner, F. X., Helas, G., Hoffer, A., Rudich, Y., Falkovich, A. H., Moura, M. A. L., da Silva Jr., R. S., Artaxo, P., Slanina, J., and Andreae, M. O.: The NH_4^+ -NO_3^- -Cl^--SO_4^{2-} -H_2O aerosol system and its gas phase precursors
1160 at a pasture site in the Amazon Basin: How relevant are mineral cations and soluble organic acids?, Journal of Geophysical Research: Atmospheres, 110, doi:10.1029/2004JD005478, 2005.

Ulrich, B.: Nutrient and acid-base budget of central european forest ecosystems, in: Effects of Acid Rain on Forest Processes, edited by: Godbold, D., and Hüttermann, A., John Wiley & Sons, New York, USA, 1–50, 1994.

UNECE: International Cooperative Program on Integrated Monitoring of Air pollution Effects on Ecosystems (ICP IM) within
1165 the framework of the Geneva Convention on Long-Range Transboundary, available at: http://www.unece.org/env/lrtap/ (last access: 14 March 2022), 2022.

Van Damme, M., Clarisse, L., Franco, B., Sutton, M. A., Erisman, J. W., Wichink Kruit, R., van Zanten, M., Whitburn, S., Hadji-Lazaro, J., Clerbaux, C. and Coheur, P.-F.: Global, regional and national trends of atmospheric ammonia derived from a decadal (2008 – 2018) satellite record, Environmental Research Letters, 16, 055017, doi: 10.1088/1748-9326/abd5e0, 2021.

1170 Van der Graaf, S. C., Kranenburg, R., Segers, A. J., Schaap, M., and Erisman, J. W.: Satellite-derived leaf area index and roughness length information for surface–atmosphere exchange modelling: a case study for reactive nitrogen deposition in north-western Europe using LOTOS-EUROS v2.0, Geoscientific Model Development, 13, 2451–2474, doi:10.5194/gmd-13-2451-2020, 2020.

Van Jaarsveld, J. A.: The Operational Priority Substances model. Description and validation of OPS-Pro 4.1., RIVM,
1175 Bilthoven, report 500045001, https://www.pbl.nl/sites/default/files/downloads/500045001.pdf (last access: 14 March 2022), 2004.

Van Oss, R., Duyzer, J., and Wyers, P.: The influence of gas-to-particle conversion on measurements of ammonia exchange over forest,Atmospheric Environment, 32, 465 – 471, doi:10.1016/S1352-2310(97)00280-X, 1998.

Van Pul, W. A. J. and Jacobs, A. F. G.: The conductance of a maize crop and the underlying soil to ozone under various
1180 environmental conditions, Boundary-Layer Meteorology, 69, 83–99, doi:10.1007/BF00713296, 1994.

Van Zanten, M. C., Sauter, F. J., Wichink Kruit, R. J., van Jaarsveld, J. A., and van Pul, W. A. J.: Description of the DEPAC module; Dry deposition modeling with DEPAC_GCN2010, Tech. rep., RIVM, Bilthoven, NL, 2010.

VDI: VDI-Guideline 3782 Part 5: Environmental meteorology – Atmospheric dispersion models – Deposition parameters, Tech. rep., Verein Deutscher Ingenieure, Düsseldorf, DE, 2006.

1185 Walker, J. T., Beachley, G., Zhang, L., Benedict, K. B., Sive, B. C., and Schwede, D. B.: A review of measurements of air-surface exchange of reactive nitrogen in natural ecosystems across North America, Science of The Total Environment, 698, 133975, doi: 10.1016/j.scitotenv.2019.133975, 2020.

Watson, L., Lacressonnière, G., Gauss, M., Engardt, M., Andersson, C., Josse, B., Marécal, V., Nyiri, A., Sobolowski, S., Siour, G., Szopa, S., and Vautard, R.: Impact of emissions and +2°C climate change upon future ozone and nitrogen dioxide
1190 over Europe, Atmospheric Environment, 142, 271-285, doi: 10.1016/j.atmosenv.2016.07.051, 2016.

Webb, E. K.: Profile relationships: The log-linear range, and extension to strong stability, Quarterly Journal of the Royal Meteorological Society, 96, 67–90, doi:10.1002/qj.49709640708, 1970.

Wentworth, G. R., Murphy, J. G., Benedict, K. B., Bangs, E. J., and Collett Jr, J. L.: The role of dew as a nighttime reservoir and morning source for atmospheric ammonia, Atmospheric Chemistry and Physics Discussions, 16, 1–36, doi:10.5194/acp-
1195 2016-169, 2016.

Whitehead, J. D., Twigg, M., Famulari, D., Nemitz, E., Sutton, M. A., Gallagher, M. W., and Fowler, D.: Evaluation of laser absorption spectroscopic techniques for eddy covariance flux measurements of ammonia, Environ Sci Technol, 42, 2041–6, doi:10.1021/es071596u, 2008.

Wichink Kruit, R. J., van Pul, W. A. J., Sauter, F. J., van den Broek, M., Nemitz, E., Sutton, M. A., Krol, M., and Holtslag, A.
1200 A.M.: Modeling the surface–atmosphere exchange of ammonia, Atmospheric Environment, 44, 945–957, doi:10.1016/j.atmosenv.2009.11.049, 2010.

Wichink Kruit, R. J., Schaap, M., Sauter, F. J., van Zanten, M. C., and van Pul, W. A. J.: Modeling the distribution of ammonia across Europe including bi-directional surface–atmosphere exchange, Biogeosciences, 9, 5261–5277, doi:10.5194/bg-9-5261-2012, 2012.

1205 Wichink Kruit, R. J., Aben, J., de Vries, W., Sauter, 1180 F., van der Swaluw, E., van Zanten, M. C., and van Pul, W. A. J.: Modelling trends in ammonia in the Netherlands over the period 1990–2014, Atmospheric Environment, 154, 20–30, doi: 10.1016/j.atmosenv.2017.01.031, 2017.

Wintjen, P., Ammann, C., Schrader, F., and Brümmer, C.: Correcting high-frequency losses of reactive nitrogen flux measurements, Atmospheric Measurement Techniques, 13, 2923–2948, doi:10.5194/amt-13-2923-2020, 2020.

1210 Wintjen, P., Schrader, F., Schaap, M., Beudert, B., and Brümmer, C.: Forest–atmosphere exchange of reactive nitrogen in a remote region – Part I: Measuring temporal dynamics, Biogeosciences, 19, 389–413, doi:10.5194/bg-19-389-2022, 2022.

Wolff, V., Trebs, I., Foken, T., and Meixner, F. X.: Exchange of reactive nitrogen compounds: concentrations and fluxes of total ammonium and total nitrate above a spruce canopy, Biogeosciences, 7, 1729–1744, doi:10.5194/bg-7-1729-2010, 2010.

Wyers, G. and Duyzer, J.: Micrometeorological measurement of the dry deposition flux of sulphate and nitrate aerosols to
1215 coniferous forest, Atmospheric Environment, 31, 333 – 343, doi:10.1016/S1352-2310(96)00188-4, 1997.

Wyers, G. P. and Erisman, J. W.: Ammonia exchange over coniferous forest, Atmospheric Environment, 32, 441–451, doi:10.1016/S1352-2310(97)00275-6, 1998.

Zhang, L., Gong, S., Padro, J., and Barrie, L.: A size-segregated particle dry deposition scheme for an atmospheric aerosol module, Atmospheric Environment, 35, 549-560, doi:10.1016/S1352-2310(00)00326-5, 2001.

1220 Zöll, U., Brümmer, C., Schrader, F., Ammann, C., Ibrom, A., Flechard, C. R., Nelson, D. D., Zahniser, M., and Kutsch, W. L.: Surface–atmosphere exchange of ammonia over peatland using QCL-based eddy-covariance measurements and inferential modeling, Atmospheric Chemistry and Physics, 16, 11 283–11 299, doi:10.5194/acp-16-11283-2016, 2016.

Zöll, U., Lucas-Moffat, A. M., Wintjen, P., Schrader, F., Beudert, B., and Brümmer, C.: Is the biosphere-atmosphere exchange of total reactive nitrogen above forest driven by the same factors as carbon dioxide? An analysis using artificial neural
1225 networks, Atmospheric Environment, 206, 108–118, doi: 10.1016/j.atmosenv.2019.02.042, 2019.